J. Fluid Mech. (1990), *vol.* 212, *pp.* 155–182
Printed in Great Britain

A new continuum model for suspensions of gyrotactic micro-organisms

By T. J. PEDLEY[1] AND J. O. KESSLER[2]
[1] Department of Applied Mathematical Studies, University of Leeds, Leeds LS2 9JT, UK
[2] Department of Physics, University of Arizona, Tucson, AZ 85721, USA

(Received 29 April 1989)

A new continuum model is formulated for dilute suspensions of swimming micro-organisms with asymmetric mass distributions. Account is taken of randomness in a cell's swimming direction, $\boldsymbol{p}$, by postulating that the probability density function for $\boldsymbol{p}$ satisfies a Fokker–Planck equation analogous to that obtained for colloid suspensions in the presence of rotational Brownian motion. The deterministic torques on a cell, viscous and gravitational, are balanced by diffusion, represented by an isotropic rotary diffusivity D_r, which is unknown *a priori*, but presumably reflects stochastic influences on the cell's internal workings. When the Fokker–Planck equation is solved, macroscopic quantities such as the average cell velocity V_c, the particle diffusivity tensor $\boldsymbol{D}$ and the effective stress tensor $\boldsymbol{\Sigma}$ can be computed; V_c and $\boldsymbol{D}$ are required in the cell conservation equation, and $\boldsymbol{\Sigma}$ in the momentum equation. The Fokker–Planck equation contains two dimensionless parameters, λ and ϵ; λ is the ratio of the rotary diffusion time D_r^{-1} to the torque relaxation time B (balancing gravitational and viscous torques), while ϵ is a scale for the local vorticity or strain rate made dimensionless with B. In this paper we solve the Fokker–Planck equation exactly for $\epsilon = 0$ (λ arbitrary) and also obtain the first-order solution for small ϵ. Using experimental data on V_c and $\boldsymbol{D}$ obtained with the swimming alga, *Chlamydomonas nivalis*, in the absence of bulk flow, the $\epsilon = 0$ results can be used to estimate the value of λ for that species ($\lambda \approx 2.2$; $D_r \approx 0.13\ \mathrm{s}^{-1}$). The continuum model for small ϵ is then used to reanalyse the instability of a uniform suspension, previously investigated by Pedley, Hill & Kessler (1988). The only qualitatively different result is that there no longer seem to be circumstances in which disturbances with a non-zero vertical wavenumber are more unstable than purely horizontal disturbances. On the way, it is demonstrated that the only significant contribution to $\boldsymbol{\Sigma}$, other than the basic Newtonian stress, is that derived from the stresslets associated with the cells' intrinsic swimming motions.

---

1. Introduction

This paper is concerned with the development of a rational continuum description of the properties of suspensions of active small particles. The aim is to be able to analyse collective behaviour and pattern formation in populations of swimming micro-organisms. Bioconvection is the term used to describe the convective instabilities that result from the swimming of micro-organisms that are slightly denser than the ambient fluid; for example, Childress, Levandowsky & Spiegel (1975) showed how pure upswimming of such organisms can result in a density stratification which is unstable by mechanisms analogous to that of Rayleigh–Bénard convection.

Kessler (1984) demonstrated that certain species of micro-organisms swim upwards in still fluid because they are bottom-heavy; this has the consequence that when a cell is swimming in a shear flow, the viscous torque exerted on it by the fluid, coupled with the gravitational torque resulting from its asymmetric mass distribution, will orient it so that its swimming direction is not in general vertical, a process known as gyrotaxis.

Gyrotaxis causes bottom-heavy cells to be concentrated in regions of downflow, and away from regions of upflow, thereby making the downflow regions denser than the upflow regions. This provides a mechanism for the instability of an initially uniform suspension, which would be stable if the cells merely swam upwards; such an instability has been demonstrated experimentally by Kessler (1986*a*), and theoretical analysis has been given by Kessler (1986*b*) and by Pedley, Hill & Kessler (1988, henceforth referred to as PHK). The final, nonlinear patterns generated after such an instability are observed to take the form of long vertical plumes, spaced a few mm apart and with fluid velocities significantly greater than the cell swimming speed (Kessler 1986*b*).

The micro-organism used in Kessler's experiments is the motile alga, *Chlamydomonas nivalis*, depicted in figure 1. The cell body is approximately a prolate spheroid, of length d about 10 μm, volume v about 500 μm^3 and major-to-minor axis ratio about 1.4. The cell density $\rho+\Delta\rho$ exceeds that of the surrounding water, ρ, by about 5 %. The cell swims by means of a pair of flagella located near one end (the 'front' end) of the major axis; these flagella operate a sort of low-Reynolds-number breast-stroke, and propel the cell at a speed V_s of around 70 μm s^{-1} relative to the ambient fluid. Many cells appear to spiral as they advance, as if the flagella exert a torque about the cell axis as well as a thrust parallel to it. Note however that *C. nivalis* is just one example; we expect that a theory of the type presented here will be applicable to a wide range of swimming micro-organisms, oriented by a variety of external influences (light, chemical gradients, etc.), not to mention certain passive bodies such as charged particles under the action of the force and couple induced by an electric field (see Baloch & van de Ven 1989).

In our model we assume a dilute suspension and neglect all cell–cell interactions. Guell *et al.* (1988) showed how cell–cell interactions could be responsible for pattern formation in suspensions of magnetotactic bacteria swimming parallel to an applied magnetic field. There the bacteria swim in bands, transverse to the magnetic field, each band moving with a speed roughly equal to the cell swimming speed, and neighbouring bands being distinguished by different swimming speeds (Spormann 1987). We cannot rule out the possibility that such an effect may be important in algal suspensions at a large enough volume fraction, but the fact that the observed fluid speeds are significantly greater than the cell swimming speed suggests that it is not dominant.

1.1. *Continuum equations*

In this paper, as in PHK and in Childress *et al.* (1975), we shall develop a continuum model for a dilute suspension of swimming cells, requiring that the volume fraction nv, where $n(\boldsymbol{x},t)$ is the number of cells per unit volume, dependent on position $\boldsymbol{x}$ and time t, be small compared with unity. The equations governing conservation of mass, momentum and cell number in such a model are

$$\nabla\cdot\boldsymbol{u}=0, \tag{1.1}$$

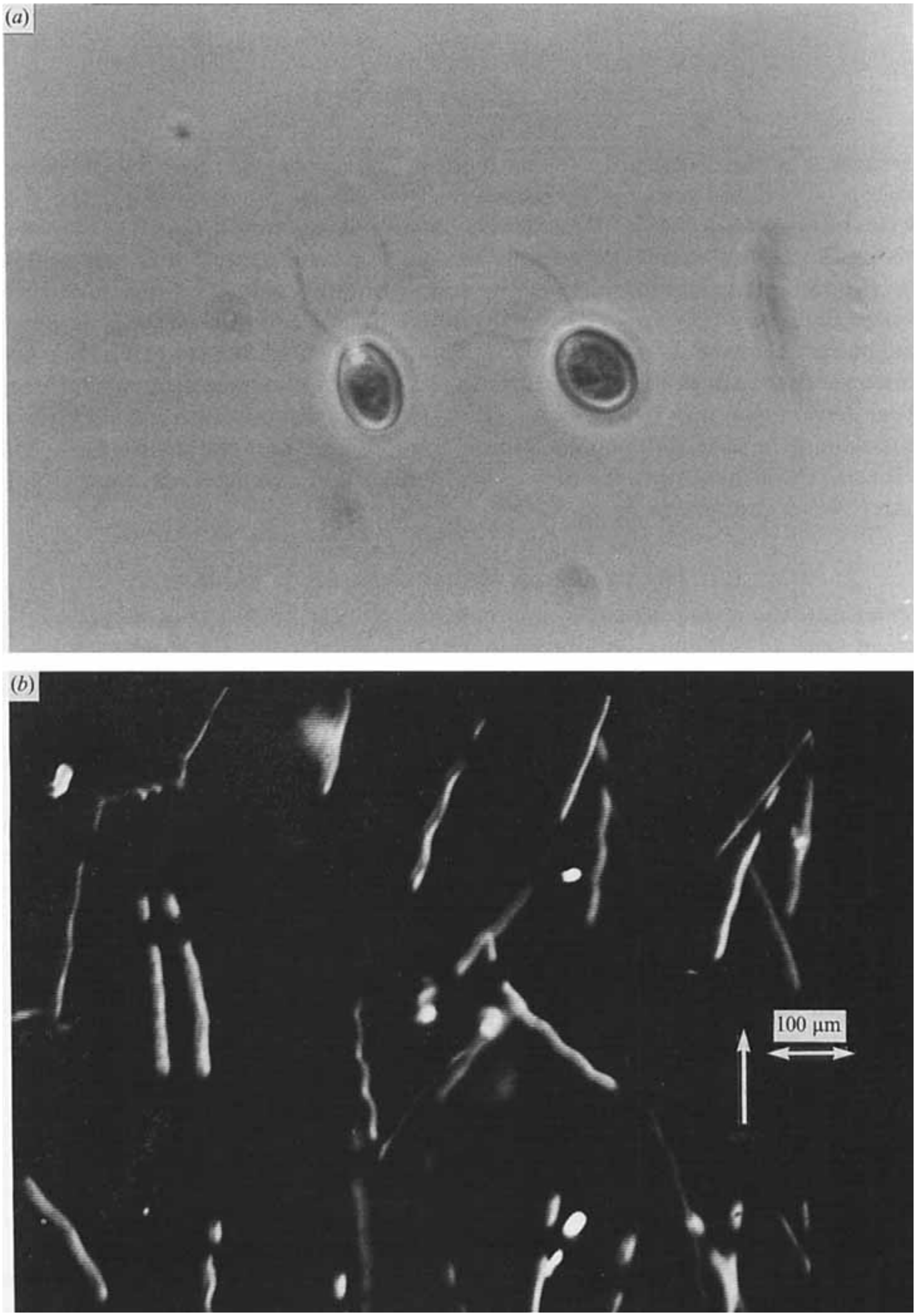

FIGURE 1. Photomicrographs of the swimming alga, *Chlamydomonas nivalis*. (*a*) Stationary and pressed between microscopic slides, so the flagella are visible (the minor axis of the cell on the left is 8 μm). (*b*) Swimming freely in a chamber 1 mm deep. The microscopic axis is horizontal, the upward direction and scale bar are indicated in the inset. The white streaks are swimming cells, seen in dark field on a TV monitor. The illumination was on for 3 s; then the shutter opened, closed and opened in rapid sequence, followed by permanent closing. The dark spot followed by a light spot at the end of a cell track indicates its direction. Note that some cells exhibit a more helical trajectory than others. The width and illumination of the tracks vary with focus.

$$\rho \frac{D\boldsymbol{u}}{Dt} = -\nabla p_e + nv\Delta\rho \boldsymbol{g} + \nabla \cdot \boldsymbol{\Sigma}, \tag{1.2}$$

$$\frac{\partial n}{\partial t} = -\nabla \cdot [n(\boldsymbol{u} + \boldsymbol{V}_c) - \boldsymbol{D} \cdot \nabla n], \tag{1.3}$$

where $\boldsymbol{u}(\boldsymbol{x}, t)$ is the Eulerian velocity field of the suspension, $\boldsymbol{g}$ is the gravitational vector, $p_e(\boldsymbol{x}, t)$ is the pressure excess above hydrostatic (at density ρ), $\boldsymbol{\Sigma}(\boldsymbol{x}, t)$ is the bulk deviatoric stress tensor, $\boldsymbol{V}_c(\boldsymbol{x}, t)$ is the mean cell swimming velocity, representing the contribution of active swimming to cell flux, and $\boldsymbol{D}(\boldsymbol{x}, t)$ is a cell diffusivity tensor, representing randomness in the cell swimming velocity (note how the cells depicted in figure 1(*b*) are not all swimming in the same direction). It has been assumed that the cells and the fluid are incompressible, leading to (1.1), that density variations do not affect the inertia term in (1.2) (the Boussinesq approximation), and that sedimentation can be neglected in (1.3) (the sedimentation velocity for these cells can be estimated to be about 3 μm s^{-1}, much less than the swimming speed V_s). We retain these assumptions here. However, other assumptions made by PHK demand closer examination.

1.2. *Randomness in the cell conservation equation*

Consider first the mean cell swimming velocity $\boldsymbol{V}_c$ in (1.3). In the previous model, we assumed that all cells in a volume element swim relative to the fluid with the same speed V_s in the same direction $\boldsymbol{p}$, where $\boldsymbol{p}(\boldsymbol{x}, t)$ is the unit vector in the direction of the cell's axis of symmetry; thus

$$\boldsymbol{V}_c = V_s \boldsymbol{p}. \tag{1.4}$$

It was further assumed that $\boldsymbol{p} = \boldsymbol{P}$, the swimming direction determined by the (quasi-) steady gyrotactic torque balance on the cell, as calculated by Pedley & Kessler (1987) using the expressions for viscous torque on a spheroid, moving at low Reynolds number in a fluid with non-zero vorticity and strain rate, given by Batchelor (1970) based on Jeffery (1922). However, we know that there is some randomness in the cells' swimming: different cells have different swimming speeds and directions (figure 1*b*), and a given cell has a variable speed and direction. If we assume that swimming speed and direction are independent stationary random variables, we can take V_s as the mean swimming speed, but in place of (1.4) we should write

$$\boldsymbol{V}_c = V_s \langle \boldsymbol{p} \rangle, \tag{1.5}$$

where $\langle\ \rangle$ represents the ensemble average (assumed to be the same as the volume average over a volume element). The previous assumption that $\boldsymbol{p} = \boldsymbol{P}$ for all cells in a volume element is equivalent to assuming that the randomness is in some sense very weak compared with gyrotaxis in determining the swimming direction.

Now consider the cell diffusivity tensor $\boldsymbol{D}$ in (1.3). Childress *et al.* (1975) recognized that vertical cell swimming would lead to anisotropy and took $\boldsymbol{D}$ to be orthotropic, with different values for vertical and horizontal diffusivities, D_V and D_H; though they had no way of estimating the ratio D_H/D_V, the results of their analysis agreed better with experiments using *Tetrahymena* if D_H were significantly less than D_V. In the absence of any knowledge of this ratio, PHK took $\boldsymbol{D}$ to be isotropic. This corresponds to assuming that the randomness is in some sense very strong compared with the gyrotactic bias. Thus the PHK model as it stands (and any other model for a suspension of swimming cells that incorporates isotropic diffusivity with some sort

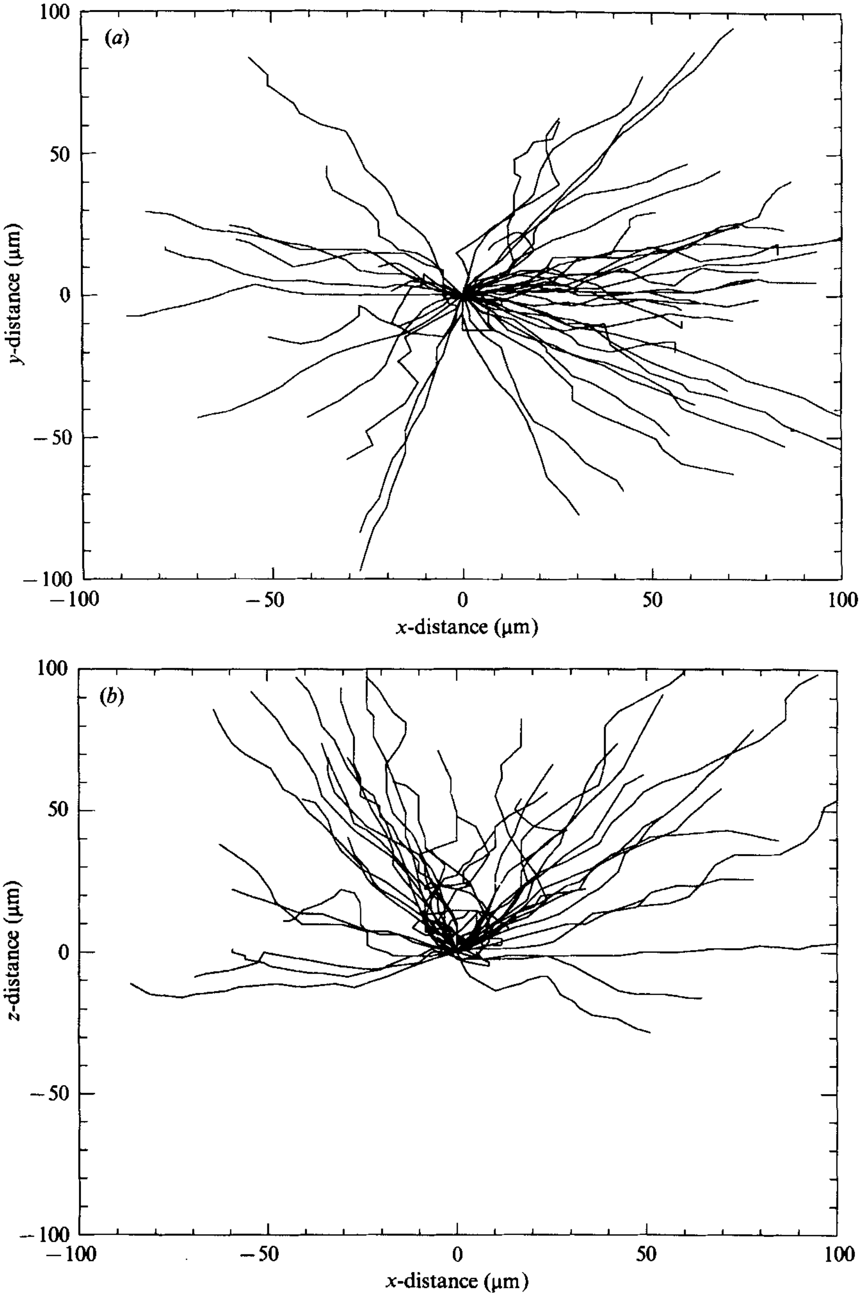

FIGURE 2. Individual trajectories of *C. nivalis*, from the measurements of Häder & Hill (1990); (*a*) horizontal projections, (*b*) vertical projections. In each case the initial points of every measured trajectory are taken to be the same.

of directed swimming, e.g., Keller & Segel 1970) is inconsistent, assuming weak randomness to specify V_c and strong randomness to specify $\boldsymbol{D}$. Of course, it would be simple to modify the PHK model to incorporate different values for D_H and D_V, but it would be important to have some knowledge of their relative magnitudes. The analysis of this paper will lead to an estimate of D_H/D_V that is greater than unity.

Moreover, data have recently been obtained on precisely this question for one particular species. Häder & Hill (1990) have plotted horizontal and vertical projections of large numbers of individual trajectories of *C. nivalis*, swimming in a fluid with no imposed ambient flow so that the only orienting mechanism is gravity, which we would expect to cause the cells to swim vertically upwards on average. They obtained results for three different values of cell concentration n_0, 5×10^5, 1×10^6 and 2×10^6 cells cm^{-3}, respectively. Even the largest of these corresponds to a volume fraction of only 10^{-3}, so the suspension can be regarded as dilute and cell–cell interactions may be supposed negligible. Examples of the projected trajectories are given in figure 2; the motion is extremely random. Preliminary analysis of the vertical projections for the lowest n_0 reveals the following quantitative data:

(i) The mean cell swimming speed, V_s, is 63 $\mu\mathrm{m\,s^{-1}}$, somewhat below the value of 100 $\mu\mathrm{m\,s^{-1}}$ estimated by Kessler (1986*a*) and used by PHK.

(ii) The mean cell *velocity* $\boldsymbol{V}_c$ has a vertical component about 10 times the horizontal component, the value of the vertical component being 32 $\mu\mathrm{m\,s^{-1}}$. Thus it is a reasonable approximation to take $\boldsymbol{V}_c = V_c\boldsymbol{k}$ ($\boldsymbol{k}$ being the upwards unit vector) with $V_c/V_s \approx 0.51$.

(iii) The effective horizontal and vertical cell diffusivities are $D_\mathrm{H} = 1.3\times10^{-5}\ \mathrm{cm^2\,s^{-1}}$ and $D_\mathrm{V} = 0.67\times10^{-5}\ \mathrm{cm^2\,s^{-1}}$, so $D_\mathrm{H}/D_\mathrm{V}\approx 1.94$, greater than one (the values of D_H and D_V are somewhat below those estimated by Kessler (1986*a*), mainly because V_s is lower than his estimate).

These data will be used below in applying our new model to suspensions of *C. nivalis*. For future reference, we also note that analysis of the horizontal projections gives a direction correlation time τ (see (1.15) below) of about 5 s.

1.3. *The bulk deviatoric stress tensor* $\boldsymbol{\Sigma}$

A further idealization of the PHK model was to ignore all effects that the cells may have on the bulk fluid motion apart from their negative buoyancy. Thus in (1.2), it was assumed that

$$\boldsymbol{\Sigma} = 2\mu\boldsymbol{E}, \tag{1.6}$$

where $\boldsymbol{E}$ is the bulk rate of strain tensor and μ is the fluid viscosity. In fact, however, there are a variety of ways in which the cells can influence the motion by modifying $\boldsymbol{\Sigma}$, even in a dilute suspension. First of all, there are 'stresslets' and 'couplets' that arise from the fact that a suspended body does not in general deform and rotate in the same way as the fluid would if the body were not there. These effects were analysed in detail by Batchelor (1970), who showed that they lead to a contribution to $\boldsymbol{\Sigma}$ of $\boldsymbol{\Sigma}^{(\mathrm{p})}$, where, for rigid spheroids whose axis of symmetry is the unit vector $\boldsymbol{p}$,

$$\begin{aligned}\boldsymbol{\Sigma}^{(\mathrm{p})} = 4\mu n v\{\alpha_1\boldsymbol{E}:\langle\boldsymbol{pppp}\rangle + \alpha_2(\boldsymbol{E}\cdot\langle\boldsymbol{pp}\rangle + \langle\boldsymbol{pp}\rangle\cdot\boldsymbol{E}) + \alpha_3\boldsymbol{E} + \alpha_4\boldsymbol{E}:\langle\boldsymbol{pp}\rangle\boldsymbol{I}\}\\ +\tfrac{1}{2}n\{\boldsymbol{\varepsilon}\cdot\langle\boldsymbol{L}\rangle + \tfrac{1}{2}\alpha_0\langle(\boldsymbol{p}\wedge\boldsymbol{L})\boldsymbol{p} + \boldsymbol{p}(\boldsymbol{p}\wedge\boldsymbol{L})\rangle\},\end{aligned} \tag{1.7}$$

where

$$\boldsymbol{L} = -\rho v h\boldsymbol{p}\wedge\boldsymbol{g} \tag{1.8}$$

is the external couple applied to the fluid by an individual cell ($-h\boldsymbol{p}$ is the displacement of the cell's centre of mass from the centre of the spheroid), $\boldsymbol{\varepsilon}$ is the alternating tensor,

$$\alpha_0 = \frac{a^2-b^2}{a^2+b^2} \tag{1.9}$$

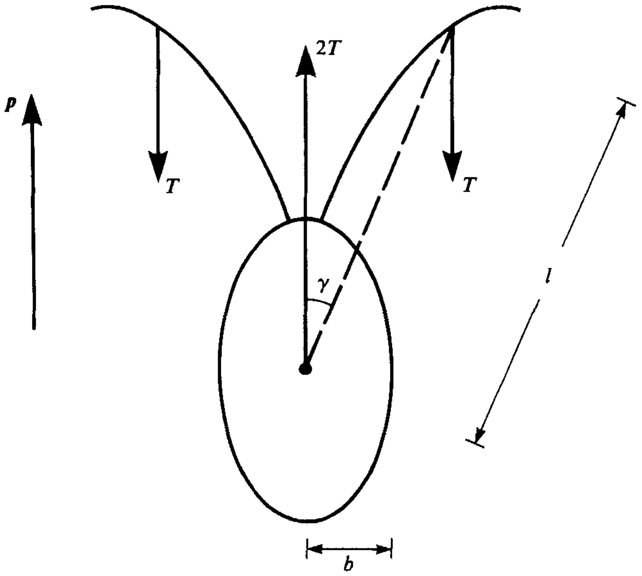

FIGURE 3. Schematic diagram of a swimming biflagellate, illustrating the calculation of its stresslet strength (see text).

is a measure of the eccentricity of the spheroid, and α_1, α_2, α_3, α_4 are further constants depending only on α_0 (see Appendix A). Note that

$$(\boldsymbol{p} \wedge \boldsymbol{L})\boldsymbol{p}+\boldsymbol{p}(\boldsymbol{p} \wedge \boldsymbol{L}) = \rho v h g[2(\boldsymbol{p}\cdot\boldsymbol{k})\boldsymbol{p}\boldsymbol{p}-\boldsymbol{k}\boldsymbol{p}-\boldsymbol{p}\boldsymbol{k}]. \tag{1.10}$$

There is a further contribution to the particle stress resulting from the effective particle rotation caused by the rotary diffusion of $\boldsymbol{p}$ in orientation space (see the discussion following (1.16) below). This is explained by Brenner (1972) and by Hinch & Leal (1972*a*), and the resulting contribution to the stress tensor is

$$\Sigma^{(d)} = 2\mu n v D_r \alpha_5(\langle \boldsymbol{p}\boldsymbol{p}\rangle - \tfrac{1}{3}\boldsymbol{I}), \tag{1.11}$$

where α_5 (called $F(r)$ by Hinch & Leal 1972*a*) depends on α_0 and is also given in Appendix A, and D_r is the rotary diffusivity, with dimensions of inverse time.

In the case of swimming cells, there is an additional stresslet contribution to the stress tensor from the locomotory motions themselves. Consider the biflagellate depicted in figure 3, and suppose that each flagellum exerts (on average) a thrust force $-T\boldsymbol{p}$ on the fluid, while the body therefore exerts a drag force $+2T\boldsymbol{p}$. For a spheroid moving with relative speed V_s parallel to its axis,

$$2T = 6\pi b \mu V_s \alpha_F, \tag{1.12a}$$

where α_F depends on the eccentricity and is given in Appendix A. If the displacements of the points of application of the thrust forces from the centre of the body (i.e. from the effective point of application of the drag) have magnitude l and are inclined (on average) at angle γ with $\boldsymbol{p}$, then, neglecting inertia, the velocity field at displacement $\boldsymbol{x}$ from the body, where $r = |\boldsymbol{x}| \gg l$, is dominated by the stresslet term (Batchelor 1970):

$$\boldsymbol{u} \sim -\frac{3}{8\pi\mu}(\boldsymbol{S}:\boldsymbol{x}\boldsymbol{x})\frac{\boldsymbol{x}}{r^3},$$

where the stresslet strength $\boldsymbol{S}$ is given by

$$\boldsymbol{S} = 2Tl\cos\gamma(\boldsymbol{pp}-\tfrac{1}{3}\boldsymbol{I}).$$

Thus the contribution to the bulk stress tensor from a volume distribution of such stresslets is given by

$$\boldsymbol{\Sigma}^{(\mathrm{s})} = nS(\langle\boldsymbol{pp}\rangle-\tfrac{1}{3}\boldsymbol{I}), \tag{1.12b}$$

where

$$S = 2Tl\cos\gamma. \tag{1.12c}$$

As remarked above, the locomotory motions also cause rotation of the cells, both as a spiralling about the axis of symmetry and as the frequent rotations about a transverse axis that contribute to the randomness in swimming direction. Such a rotation is a consequence of a torque, $\boldsymbol{G}$ say, exerted by the flagella and will be balanced (since the cell Reynolds number is assumed to be zero) by an equal and opposite resistive torque $-\boldsymbol{G}$ exerted by the cell body. Thus the net torque is zero and these motions do not contribute to the bulk stress tensor, unlike the external torque $\boldsymbol{L}$ which appears in (1.7).

In summary, therefore, we shall take the total deviatoric stress tensor to be the sum of the contributions given by (1.6), (1.7), (1.11), and (1.12*b*):

$$\boldsymbol{\Sigma} = 2\mu\boldsymbol{E}+\boldsymbol{\Sigma}^{(\mathrm{p})}+\boldsymbol{\Sigma}^{(\mathrm{d})}+\boldsymbol{\Sigma}^{(\mathrm{s})}. \tag{1.13}$$

It should be remarked (*a*) that it may not be consistent to treat $\boldsymbol{\Sigma}^{(\mathrm{s})}$ and $\boldsymbol{\Sigma}^{(\mathrm{p})}$ as purely additive, and (*b*) that there are at least three further contributions that may be important in practice, but are ignored here. The first is cell–cell interaction, negligible only if the suspension is sufficiently dilute; another is the effect of the flagella on $\boldsymbol{\Sigma}^{(\mathrm{p})}$, here calculated on the assumption that the cells are pure spheroids; and the third is the influence of the flagella on the gyrotactic torque balance that is used to calculate $\boldsymbol{V}_\mathrm{c}$ (equation (1.5)) and other average quantities. The last two effects require a detailed study of the low-Reynolds-number locomotion of biflagellates, beyond the scope of this paper. It fortunately turns out that, for the parameter values appropriate to *C. nivalis*, the quantities $\boldsymbol{\Sigma}^{(\mathrm{p})}$ and $\boldsymbol{\Sigma}^{(\mathrm{d})}$ are negligibly small so errors in computing them are unimportant. They are retained in the analysis in case features such as the asymmetry of $\boldsymbol{\Sigma}^{(\mathrm{p})}$ introduce qualitatively new effects into the results (see §4).

1.4. *Basis of the new model*

The aim of this paper is to reformulate the continuum model for a dilute suspension, incorporating random swimming behaviour from the start, and not neglecting the effect of the cells on $\boldsymbol{\Sigma}$. We shall also use the new model to reanalyze the stability of a uniform suspension, as in PHK, to see how the newly included effects alter the conclusions.

The method will be as follows: we suppose that, in the absence of all torques, either viscous or gravitational (i.e. the cells are in a stationary fluid at zero $\boldsymbol{g}$), the cells swim in totally random directions, so that the cell swimming direction $\boldsymbol{p}$ is a stationary random variable with isotropic probability density function (p.d.f.), $f(\boldsymbol{p}) = 1/4\pi$. Thus in this case $\langle\boldsymbol{p}\rangle$, defined by

$$\langle\boldsymbol{p}\rangle \equiv \iint \boldsymbol{p}f(\boldsymbol{p})\,\mathrm{d}^2\boldsymbol{p}, \tag{1.14}$$

where the integral is over the surface of the unit sphere in $\boldsymbol{p}$-space, is zero; also $\boldsymbol{V}_c$, given by (1.5), is zero. Moreover the cell diffusivity tensor $\boldsymbol{D}$ is defined by

$$\boldsymbol{D}(t) = \int_0^\infty \langle \boldsymbol{V}_r(t)\, \boldsymbol{V}_r(t-t')\rangle\, \mathrm{d}t',$$

where $\boldsymbol{V}_r$ is the velocity of a cell relative to its mean value. Thus, if V_s is a constant we have

$$\boldsymbol{D} = V_s^2 \tau \langle (\boldsymbol{p}-\langle \boldsymbol{p}\rangle)(\boldsymbol{p}-\langle \boldsymbol{p}\rangle)\rangle,$$

independent of time t, where τ is the direction correlation time, or

$$\boldsymbol{D} = V_s^2 \tau \left[\iint \boldsymbol{p}\boldsymbol{p} f(\boldsymbol{p})\, \mathrm{d}^2\boldsymbol{p} - \langle \boldsymbol{p}\rangle \langle \boldsymbol{p}\rangle \right]: \tag{1.15}$$

this gives the tensorial character of $\boldsymbol{D}$ even if τ is unknown. If V_s is itself a random variable we might expect some modification of (1.15), but that has not yet been investigated. In the absence of gravity or flow, $\boldsymbol{D}$ is isotropic:

$$\boldsymbol{D} = \tfrac{1}{3} V_s^2 \tau \boldsymbol{I},$$

where $\boldsymbol{I}$ is the identity tensor.

In the presence of gravity and flow, however, gyrotaxis occurs and there will be a bias in $f(\boldsymbol{p})$. Cells will still perform their random swimming motions, but whatever their instantaneous direction $\boldsymbol{p}$, there will be a tendency for reorientation towards the local equilibrium direction $\boldsymbol{P}$. Assuming that the intrinsic tendency for the cells to change direction randomly is independent of the instantaneous direction, the situation may be taken to be analogous to that of small particles in suspension subjected to rotary Brownian motion, and we shall model it accordingly. It should be emphasized that this is not a case of thermal Brownian motion, since the cells are too big and move too quickly to be influenced by that, but we are treating it analogously. Thus we can make use of all the theory already developed for such suspensions, for example, by Brenner (1974) and by Hinch & Leal (1972*a*), etc. The p.d.f. $f(\boldsymbol{p})$ must satisfy the Fokker–Planck equation (representing conservation of probability density):

$$\frac{\partial f}{\partial t} + \nabla \cdot (\dot{\boldsymbol{p}} f) = D_r \nabla^2 f, \tag{1.16}$$

where ∇ is the gradient operator in two-dimensional $\boldsymbol{p}$-space and $\dot{\boldsymbol{p}}$ is the rate of change of $\boldsymbol{p}$, determined by the balance of viscous and gravitational torques to be

$$\dot{\boldsymbol{p}} = B^{-1}[\boldsymbol{k} - (\boldsymbol{k}\cdot\boldsymbol{p})\boldsymbol{p}] + \boldsymbol{\Omega} \wedge \boldsymbol{p} + 2\alpha_0 \boldsymbol{p}\cdot\boldsymbol{E}\cdot(\boldsymbol{I} - \boldsymbol{p}\boldsymbol{p}) \tag{1.17}$$

(this expression is a combination of those given by Leal & Hinch 1972 and Hinch & Leal 1972*b*, both essentially derived from Jeffery 1922). Here the only undefined quantities are $\boldsymbol{\Omega}$, the ambient vorticity, and

$$B = \frac{\mu \alpha_\perp}{2h\rho g}, \tag{1.18}$$

which is the timescale for reorientation of a cell by the gravitational torque against the resisting viscous torque ($\alpha_\perp$ is the dimensionless resistance coefficient for rotation about an axis perpendicular to $\boldsymbol{p}$, defined in Appendix A); B is also the 'gyrotactic orientation parameter' of Pedley & Kessler (1987).

The quantity D_r in (1.16) is a rotational diffusivity with dimensions of inverse time. In the case of thermal Brownian motion at temperature T,

$$D_r = \frac{\bar{k}T}{\mu v \alpha_\perp}, \tag{1.19}$$

where $\bar{k}$ is Boltzmann's constant, but since in our case we have no *a priori* notion of what '$\bar{k}T$' must be, we leave D_r as an unknown constant. Its value for *Chlamydomonas nivalis* can be estimated from the data of Häder & Hill (1990); see below.

We assume that, even in time-dependent flows, f is a stationary function, i.e. $\partial f/\partial t$ is negligible in (1.16). This is equivalent to assuming that D_r^{-1} is much less than the timescale for variation of the flow, so we need to check later that D_r is indeed much larger than the growth rate of instabilities. In §2 we shall solve the steady form of (1.16) for the case in which there is no flow, but gravity is important; there is then just the one dimensionless parameter,

$$\lambda = (BD_r)^{-1}. \tag{1.20}$$

The result for $f(\boldsymbol{p})$ will then be used to compute the average quantities $\langle \boldsymbol{p} \rangle$ and $\boldsymbol{D}$ (equations (1.14) and (1.15)); these will be directly comparable with the data of Häder & Hill (1990), and we shall be able to infer the values of λ and hence D_r for their suspension of *C. nivalis*. We shall also compute all averages required for $\boldsymbol{\Sigma}$ (equations (1.7), (1.11) and (1.12*b*)) in this limit of zero flow. In §3 we shall go on to compute the first-order correction to $f(\boldsymbol{p})$ required by the presence of a weak ambient flow for which $B\omega \ll 1$, where ω is a scale for vorticity and strain rate. This is a severe restriction for the modelling of fully developed bioconvection patterns, but is appropriate for the linear stability analysis to which the model is first going to be applied. The corresponding corrections to $\langle \boldsymbol{p} \rangle$, $\boldsymbol{D}$ and $\boldsymbol{\Sigma}$ will also be computed, but since in the context of the stability analysis $\boldsymbol{\Omega}$ and $\boldsymbol{E}$ are already first-order small quantities, we do not need to compute the corrections to the averages involving them in (1.7). That is a considerable simplification. The stability problem is solved in §4, and a discussion of desirable future developments of the theory is given in §5.

2. The case of pure gravity, no flow

The Fokker–Planck equation (1.16), with $\partial f/\partial t = 0$ and with $\dot{\boldsymbol{p}}$ given by (1.17), can be written

$$\lambda^{-1}\nabla^2 f = \boldsymbol{k}\cdot\nabla f - 2(\boldsymbol{k}\cdot\boldsymbol{p})f + \epsilon\{\boldsymbol{\omega}\cdot(\boldsymbol{p} \wedge \nabla f) + 2\alpha_0(\boldsymbol{p}\cdot\boldsymbol{e}\cdot\nabla f - 3\boldsymbol{p}\cdot\boldsymbol{e}\cdot\boldsymbol{p}f)\}, \tag{2.1}$$

where λ is given by (1.20), $\boldsymbol{\omega}$ and $\boldsymbol{e}$ are the vorticity and rate of strain made dimensionless with the scale ω, and

$$\epsilon = B\omega. \tag{2.2}$$

The value of λ is arbitrary, but we shall take $\epsilon \ll 1$; this is the limit discussed, for example, in Appendix C of Brenner & Weissman (1972) during their analysis of a suspension of spherical cells subjected to external couples. In this section we shall take $\epsilon = 0$, with $O(\epsilon)$ corrections calculated in §3.

Throughout the paper, we shall use a coordinate system fixed in the laboratory frame with the 3-axis vertically upwards, parallel to $\boldsymbol{k}$. The unit vector $\boldsymbol{p}$ is represented by Euler angles θ, ϕ with $\boldsymbol{p}\cdot\boldsymbol{k} = \cos\theta$. Brenner & Weissman (1972) took the 3-axis parallel to the local vorticity vector, but that is both cumbersome and inapplicable in the absence of ambient flow. Putting $\epsilon = 0$ in (2.1) and taking

$$\boldsymbol{p} = (\sin\theta\cos\phi, \sin\theta\sin\phi, \cos\theta), \tag{2.3}$$

the equation for f becomes

$$\frac{1}{\sin\theta}\frac{\partial}{\partial\theta}\left(\sin\theta\frac{\partial f}{\partial\theta}\right)+\frac{1}{\sin^2\theta}\frac{\partial^2 f}{\partial\phi^2} = -\lambda\left(\sin\theta\frac{\partial f}{\partial\theta}+2\cos\theta f\right). \tag{2.4}$$

This must be solved subject to the requirements that f should be positive and finite, should tend to the isotropic solution $1/4\pi$ as $\lambda \rightarrow 0$ (i.e. as randomness dominates gravity), and should obey the normalization condition

$$\int_0^{2\pi}\int_0^{\pi} f(\theta,\phi)\sin\theta\,\mathrm{d}\theta\,\mathrm{d}\phi = 1. \tag{2.5}$$

These requirements show that f is independent of ϕ, and the appropriate solution of (2.4) is

$$f = f^{(0)}(\theta) \equiv \mu\,\mathrm{e}^{\lambda\cos\theta}, \tag{2.6}$$

where
$$\mu = \lambda/(4\pi\sinh\lambda) \tag{2.7}$$

(Brenner & Weissman 1972).

We first compute the zero-order (in ϵ) average quantities required in the cell conservation equation (1.3). From (1.14) we have

$$\langle\boldsymbol{p}\rangle^{(0)} = (0, 0, \coth\lambda - 1/\lambda), \tag{2.8}$$

which is vertically upwards as expected and gives $|V_c|/V_s$, from (1.5), as

$$V_c/V_s = \coth\lambda - 1/\lambda = K_1 \quad \text{(say)}. \tag{2.9}$$

This quantity approximates to $\frac{1}{3}\lambda$ as $\lambda \rightarrow 0$, and $1-1/\lambda$ as $\lambda \rightarrow \infty$, confirming that there is no net drift velocity if randomness dominates gravity, and $V_c \sim V_s$ when randomness is negligible, so all cells swim vertically upwards with speed V_s.

To evaluate $\boldsymbol{D}^{(0)}$, we require $\langle\boldsymbol{pp}\rangle^{(0)}$, which is a diagonal tensor with

$$\langle\boldsymbol{pp}\rangle^{(0)}_{11} = \langle\boldsymbol{pp}\rangle^{(0)}_{22} = K_1/\lambda, \quad \langle\boldsymbol{pp}\rangle^{(0)}_{33} = 1-2K_1/\lambda. \tag{2.10a, b}$$

Thus, from (1.15), we have that $\boldsymbol{D}^{(0)}$ is also diagonal, with

$$D^{(0)}_{11} = D^{(0)}_{22}(=D_{\mathrm{H}}) = V_s^2\tau K_1/\lambda, \quad D^{(0)}_{33} = (D_{\mathrm{V}}) = V_s^2\tau K_2 \tag{2.11a, b}$$

where
$$K_2 = 1-\coth^2\lambda + 1/\lambda^2; \tag{2.11c}$$

thus
$$D_{\mathrm{H}}/D_{\mathrm{V}} = K_1/\lambda K_2, \tag{2.12}$$

which tends to $1+2\lambda^2/15$ as $\lambda \rightarrow 0$ and to $\lambda(1-1/\lambda)$ as $\lambda \rightarrow \infty$. As shown by the above results of Häder & Hill (1990), the quantities given in (2.9) and (2.12) can be measured; a test of the present model is therefore to see if the same value of λ is given by each measurement. In figure 4 we plot V_c/V_s aganist $D_{\mathrm{H}}/D_{\mathrm{V}}$, and mark on it the point taken from the data ($V_c/V_s = 0.51$, $D_{\mathrm{H}}/D_{\mathrm{V}} = 1.94$). This point lies quite near the theoretical curve, which is encouraging. The value of λ corresponding to $V_c/V_s = 0.51$ is 1.85, while that corresponding to $D_{\mathrm{H}}/D_{\mathrm{V}} = 1.94$ is 2.63; the corresponding points are marked on figure 4. A particular value is needed in order to apply the present theory; we (somewhat arbitrarily) choose the average of the above numbers, rounded off to two significant figures: $\lambda = 2.2$; this point is also marked on figure 4.

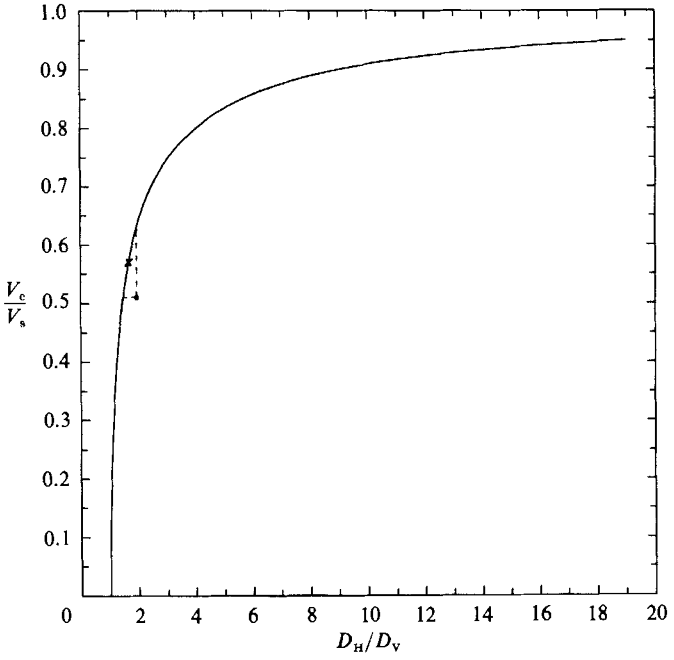

FIGURE 4. Plot of V_c/V_s versus D_H/D_V, for algae swimming in a gravitational field with no flow, as calculated from (2.9) and (2.12). The filled circle is the experimental point from the data of Häder & Hill (1989). The cross on the curve is the point chosen for estimation of λ (see text).

We may note that, since the data for *C. nivalis* listed in PHK give $B \approx 3.4$ s, this value for λ indicates a value of $D_r \approx 0.13\ \mathrm{s}^{-1}$, from (1.20).

The measured value of D_H reported above is $1.3 \times 10^{-5}\ \mathrm{cm}^2\ \mathrm{s}^{-1}$. Coupled with the measured value of V_s of 63 μm s^{-1} and the calculated value of $K_1/\lambda = 0.26$ for $\lambda = 2.2$, (2.11*a*) gives a direction correlation time τ equal to 1.3 s, significantly shorter than the observational estimate of 5 s. The source of this discrepancy is unknown, although Häder & Hill (1990) suggest that the estimate of diffusivity is more certain than that of τ. Where needed below, therefore, we shall use $\tau = 1.3$ s.

We now list the average quantities needed for the bulk stress tensor; their values for the experimental value of λ of 2.2 are given in table 1 below or in square brackets after the relevant equation. From (1.11), (1.12) and (2.10) we have that $\Sigma^{(d)(0)}$ and $\Sigma^{(s)(0)}$ are diagonal. Writing

$$\Sigma^{(sd)} = \Sigma^{(s)} + \Sigma^{(d)} \quad \text{and} \quad S' = S + 2\mu v D_r \alpha_5 \tag{2.13}$$

we have
$$\Sigma^{(sd)(0)}_{11} = \Sigma^{(sd)(0)}_{22} = -\tfrac{1}{2}\Sigma^{(sd)(0)}_{33} = -\tfrac{1}{3}nS'K_3, \tag{2.14a}$$

where
$$K_3 = 1 - 3K_1/\lambda. \tag{2.14b}$$

In (1.7) the first term involving the couple $\boldsymbol{L}$ is $\langle \boldsymbol{L} \rangle^{(0)}$, which is zero; the next term, $\frac{1}{4}n\alpha_0\langle(\boldsymbol{p} \wedge \boldsymbol{L})\boldsymbol{p} + \boldsymbol{p}(\boldsymbol{p} \wedge \boldsymbol{L})\rangle^{(0)}$ can be evaluated using (1.10), and is also a diagonal tensor, $\Sigma^{(L)(0)}$ say, such that

$$\Sigma^{(L)(0)}_{11} = \Sigma^{(L)(0)}_{22} = -\tfrac{1}{2}\Sigma^{(L)(0)}_{33} = \tfrac{1}{2}n\alpha_0 \rho v h g K_3/\lambda. \tag{2.15}$$

In view of (2.10), the only term in (1.7) that remains to be evaluated is $\langle \boldsymbol{pppp} \rangle^{(0)}$, which we will denote by C_{ijkl}. We see that $C_{ijkl} = 0$ if any three of $(ijkl)$ are the same and different from the fourth or if only two of $(ijkl)$ are the same. Otherwise, if $(ijkl) = (1122)$ in any order, then

$$3C_{ijkl} = C_{1111} = C_{2222} = 3K_3/\lambda^2\,[=0.14], \tag{2.16a}$$

if $(ijkl) = (1133)$ or (2233) in any order, then

$$C_{ijkl} = -\frac{1}{\lambda}\left[\frac{1}{\lambda}\left(5+\frac{12}{\lambda^2}\right)-\coth\lambda\left(1+\frac{12}{\lambda^2}\right)\right][=0.076]; \tag{2.16b}$$

finally

$$C_{3333} = \left[1+\frac{12}{\lambda^2}+\frac{24}{\lambda^4}-\frac{4\coth\lambda}{\lambda}\left(1+\frac{6}{\lambda^2}\right)\right][=0.33]. \tag{2.16c}$$

3. First-order corrections for weak ambient flow

When $\epsilon \ll 1$ we may set $f = f^{(0)}(\theta)+\epsilon f^{(1)}$ in the Fokker–Planck equation (2.1), and in terms of our Euler angles the equation for $f^{(1)}(\theta,\phi)$ becomes

$$\frac{1}{\sin\theta}\frac{\partial}{\partial\theta}\left(\sin\theta\frac{\partial f^{(1)}}{\partial\theta}\right)+\frac{1}{\sin^2\theta}\frac{\partial^2 f^{(1)}}{\partial\phi^2}+\frac{\lambda}{\sin\theta}\frac{\partial}{\partial\theta}(\sin^2\theta f^{(1)})$$
$$= \lambda(\omega_2\cos\phi-\omega_1\sin\phi)\frac{\mathrm{d}f^{(0)}}{\mathrm{d}\theta}+2\lambda\alpha_0\left(\boldsymbol{p}\cdot\boldsymbol{e}\cdot\boldsymbol{e}_\theta\frac{\mathrm{d}f^{(0)}}{\mathrm{d}\theta}-3\boldsymbol{p}\cdot\boldsymbol{e}\cdot\boldsymbol{p}f^{(0)}\right), \tag{3.1}$$

where we have used the fact that $\partial f^{(0)}/\partial\phi \equiv 0$ and where

$$\boldsymbol{e}_\theta = (\cos\theta\cos\phi,\, \cos\theta\sin\phi,\, -\sin\theta)$$

is the unit vector in the direction of increasing θ. The coefficients in the last term of (3.1) are

$$\boldsymbol{p}\cdot\boldsymbol{e}\cdot\boldsymbol{e}_\theta = -\tfrac{3}{4}e_{33}\sin 2\theta+\tfrac{1}{4}(e_{11}-e_{22})\sin 2\theta\cos 2\phi$$
$$+\tfrac{1}{2}e_{12}\sin 2\theta\sin 2\phi+e_{13}\cos 2\theta\cos\phi+e_{23}\cos 2\theta\sin\phi \tag{3.2}$$

and

$$\boldsymbol{p}\cdot\boldsymbol{e}\cdot\boldsymbol{p} = \tfrac{1}{2}e_{33}(3\cos^2\theta-1)+\tfrac{1}{2}(e_{11}-e_{22})\sin^2\theta\cos 2\phi$$
$$+e_{12}\sin^2\theta\sin 2\phi+e_{13}\sin 2\theta\cos\phi+e_{23}\sin 2\theta\sin\phi, \tag{3.3}$$

where we have used the identity $e_{ii} = 0$, from incompressibility.

3.1. *Spherical cells*

For spherical cells $\alpha_0 = 0$, the rate-of-strain tensor does not influence $f(\boldsymbol{p})$, and (3.1) is considerably simplified. This is the case treated by Brenner & Weissman (1972), but not all quantities of interest here were evaluated in their Appendix C. Making the transformation $x = \cos\theta$ and writing

$$f^{(1)}(\theta,\phi) = \lambda\mu(\omega_2\cos\phi-\omega_1\sin\phi)\,g_1(x),$$

we obtain

$$\frac{\mathrm{d}}{\mathrm{d}x}[(1-x^2)g_1']-\frac{g_1}{1-x^2}-\lambda\frac{\mathrm{d}}{\mathrm{d}x}[(1-x^2)g_1] = -\lambda(1-x^2)^{\frac{1}{2}}\mathrm{e}^{\lambda x}, \tag{3.4}$$

where a prime denotes differentiation with respect to x.

The first two terms of (3.4) suggest that we express the solution as a series of associated Legendre functions, $P_r^1(x) = (1-x^2)^{\frac{1}{2}}\,\mathrm{d}P_r(x)/\mathrm{d}x$, but it proves convenient to expand first in powers of λ. Thus we write

$$g_1 = \sum_{n=1}^{\infty} \lambda^n G_n(x),$$

so that
$$\frac{\mathrm{d}}{\mathrm{d}x}[(1-x^2)\,G'_{n+1}] - \frac{G_{n+1}}{1-x^2} = \frac{\mathrm{d}}{\mathrm{d}x}[(1-x^2)\,G_n] - \frac{(1-x^2)^{\frac{1}{2}}x^n}{n!}, \tag{3.5}$$

and then set
$$G_n(x) = \sum_{r=1}^{n} a_{n,r} P_r^1(x). \tag{3.6}$$

Substitution of this last expression into (3.5), using the standard recurrence relations for the P_r^1 (see Arfken 1985, p. 669) yields the following recurrence relation for the $a_{n,r}$:

$$a_{n+1,r} = -a_{n,r+1}\frac{r+2}{(r+1)(2r+3)} + a_{n,r-1}\frac{r-1}{r(2r-1)} + \frac{b_{n+1,r}}{r(r+1)}, \tag{3.7a}$$

where

$$b_{n+1,r} = \frac{(2r+1)}{n!\,2r(r+1)}\int_{-1}^{1}(1-x^2)^{\frac{1}{2}}x^n P_r^1(x)\,\mathrm{d}x \quad (n = 1, 2, \ldots; \quad 1 \leqslant r \leqslant n+1). \tag{3.7b}$$

Thus
$$\begin{aligned} b_{n+1,r} &= 0 \quad \text{if } n+r \text{ is even} \\ &= +\frac{(2r+1)\,\Gamma\left(\dfrac{n+1}{2}\right)\Gamma\left(\dfrac{n+2}{2}\right)}{4\Gamma(n+1)\,\Gamma\left(\dfrac{n-r+3}{2}\right)\Gamma\left(\dfrac{n+r+4}{2}\right)} \quad \text{if } n+r \text{ is odd;} \end{aligned} \tag{3.8}$$

the formula for the integral in (3.7) is given by Gradshteyn & Ryzhik (1980, p. 799).† It follows that $a_{n+1,r}$ is also zero if $n+r$ is even. The leading non-zero coefficients in the series for G_n are

$$a_{1,1} = \tfrac{1}{2}, \quad a_{2,2} = \tfrac{5}{36}. \quad a_{3,1} = \tfrac{1}{120}, \quad a_{3,3} = \tfrac{13}{540};$$

higher terms can be computed readily when needed.

We can now compute the first-order corrections to $\langle \boldsymbol{p}\rangle$, $\langle \boldsymbol{pp}\rangle$, etc. Writing $\langle \boldsymbol{p}\rangle = \langle \boldsymbol{p}\rangle^{(0)} + \epsilon\langle \boldsymbol{p}\rangle^{(1)} + \ldots$, etc., we obtain

$$\langle \boldsymbol{p}\rangle^{(1)} = (\omega_2, -\omega_1, 0)\,J_1, \tag{3.9a}$$

where
$$J_1 = \pi\lambda\mu\int_{-1}^{1}(1-x^2)^{\frac{1}{2}}g_1(x)\,\mathrm{d}x = \tfrac{4}{3}\pi\lambda\mu\sum_{l=0}^{\infty}\lambda^{2l+1}a_{2l+1,1}. \tag{3.9b}$$

Moreover $\langle \boldsymbol{pp}\rangle_{ij}^{(1)}$ is non-zero only when $i,j = 1,3$ or $2,3$ in some order:

$$\langle \boldsymbol{pp}\rangle_{13}^{(1)} = \omega_2 J_2; \quad \langle \boldsymbol{pp}\rangle_{23}^{(2)} = -\omega_1 J_2, \tag{3.10a}$$

where
$$J_2 = \pi\lambda\mu\int_{-1}^{1}x(1-x^2)^{\frac{1}{2}}g_1(x)\,\mathrm{d}x = \tfrac{4}{5}\pi\lambda\mu\sum_{l=1}^{\infty}\lambda^{2l}a_{2l,2}. \tag{3.10b}$$

---

† The definition of $P_r^m(x)$ given by Gradshteyn & Ryzhik (1980) is $(-1)^m$ times that given by Arfken (1985).

The quantity $\langle 2(\boldsymbol{p}\cdot\boldsymbol{k})\boldsymbol{pp}-\boldsymbol{kp}-\boldsymbol{pk}\rangle^{(1)}$, required in (1.7) from (1.10) when $\alpha_0 \neq 0$, is also a symmetric tensor B_{ij} with the only non-zero elements being

$$B_{13} = \omega_2(J_3-J_1), \quad B_{23} = -\omega_1(J_3-J_1), \tag{3.11a}$$

where
$$J_3 = \pi\lambda\mu \int_{-1}^{1} x^2(1-x^2)^{\frac{1}{2}} g_1(x)\,\mathrm{d}x = \tfrac{16}{35}\pi\lambda\mu \sum_{l=1}^{\infty} \lambda^{2l+1} a_{2l+1,3} + \tfrac{1}{5}J_1. \tag{3.11b}$$

The coefficients $a_{n,r}$ turn out to decrease rapidly as n increases. For example, when $l \geqslant 4$, the terms $a_{2l+1,1}$ alternate in sign and $|a_{2l+1,1}/a_{2l-1,1}|$ is somewhat less than 0.1; similar results are obtained for $a_{2l,2}$ and $a_{2l,3}$. Thus the power series for J_1, J_2, J_3 not only converge, but are asymptotically useful without further manipulation for $\lambda \lesssim \surd 10$. The same is true for the power series which define other constants J_i $(i = 4, 5, \ldots, 8)$. Values of all these constants, and the constants K_i $(i = 1, 2, \ldots, 8)$ defined above and below, are given in table 1 for four values of λ: 0.3, 1.0, 3.0 and the experimental value, 2.2.

The above quantitative results have the following implications for the physical quantities defined in §1. First, the mean swimming direction $\langle \boldsymbol{p}\rangle$ is found from (2.8) and (3.9a) to be

$$\langle \boldsymbol{p}\rangle = (\epsilon J_1\omega_2, -\epsilon J_1\omega_1, K_1).$$

This should be compared with the direction $\boldsymbol{P}$ in the deterministic case when there is no randomness, the solution of (1.17) with $\dot{\boldsymbol{p}} = 0$. To first order in ϵ, with $\alpha_0 = 0$, this is

$$\boldsymbol{P} = (\epsilon\omega_2, -\epsilon\omega_1, 1).$$

It can be seen, therefore, that to this order, $\langle \boldsymbol{p}\rangle$ is in the same plane as $\boldsymbol{P}$, but the angle it makes with the vertical is smaller by the factor J_1/K_1, equal to approximately 0.80 for *C. nivalis* (from table 1).

The diffusivity tensor is obtained to first order from (1.15), (2.8), (2.11), (3.9a) and (3.10a) to be

$$\frac{\boldsymbol{D}}{V_s^2\tau} = \begin{pmatrix} K_1/\lambda & 0 & \epsilon\omega_2(J_2-K_1J_1) \\ 0 & K_1/\lambda & -\epsilon\omega_1(J_2-K_1J_1) \\ \epsilon\omega_2(J_2-K_1J_1) & -\epsilon\omega_1(J_2-K_1J_1) & K_2 \end{pmatrix}; \tag{3.12}$$

when $\lambda = 2.2$ then
$$\frac{\boldsymbol{D}}{V_s^2\tau} = \begin{pmatrix} 0.26 & 0 & -0.10\epsilon\omega_2 \\ 0 & 0.26 & 0.10\epsilon\omega_1 \\ -0.10\epsilon\omega_2 & 0.10\epsilon\omega_1 & 0.16 \end{pmatrix}.$$

The interesting point about (3.12) is that none of $\boldsymbol{k}$, $\langle \boldsymbol{p}\rangle$, or $\boldsymbol{P}$ is an eigenvector of $\boldsymbol{D}$, even to this order, so that the diffusion tensor has no axis of symmetry aligned with the vertical, the drift velocity $\boldsymbol{V}_c$ or the deterministic gyrotactic orientation $\boldsymbol{P}$. (One eigenvector *is* perpendicular to the vertical plane containing $\boldsymbol{P}$ and $\langle \boldsymbol{p}\rangle$.)

The first-order corrections to the stress tensor can also be obtained simply. The correction to $\boldsymbol{\Sigma}^{(\mathrm{sd})}$ (equation (2.13)) is merely $nS'\langle \boldsymbol{pp}\rangle^{(1)}$, given in (3.10). The correction to $\boldsymbol{\Sigma}^{(\mathrm{p})}$ involving $\boldsymbol{L}$ contains an antisymmetric term and a symmetric term, the latter strictly being zero when $\alpha_0 = 0$, but we quote it since it involves the contribution to $f^{(1)}$ involving $\boldsymbol{\omega}$ and not $\boldsymbol{e}$; from (1.7), (3.9a) and (3.11), we have

$$\boldsymbol{\Sigma}^{(\mathrm{p})(1)} = \tfrac{1}{2}n\rho vhg\left[J_1\begin{pmatrix} 0 & 0 & \omega_2 \\ 0 & 0 & -\omega_1 \\ -\omega_2 & \omega_1 & 0 \end{pmatrix} + \tfrac{1}{2}\alpha_0(J_3-J_1)\begin{pmatrix} 0 & 0 & \omega_2 \\ 0 & 0 & -\omega_1 \\ \omega_2 & -\omega_1 & 0 \end{pmatrix}\right] \tag{3.13}$$

λ	K_1	J_1	K_2	J_2	K_3	J_3	K_4	J_4	K_5	J_5	K_6	J_6	K_7	J_7	K_8	J_8
0.3	0.099	0.015	0.33	0.00074	0.0059	0.0030	−11.5	−0.0060	−0.013	−0.020	−0.0034	−0.040	0.26	−0.0051	−0.067	−0.0034
1.0	0.31	0.14	0.28	0.024	0.061	0.031	−1.35	−0.064	−0.048	−0.064	−0.033	−0.12	0.21	−0.054	−0.069	−0.034
2.2	0.57	0.45	0.16	0.16	0.22	0.12	−0.57	−0.26	−0.11	−0.13	−0.11	−0.20	0.065	−0.21	−0.076	−0.12
3.0	0.67	0.60	0.10	0.27	0.33	0.20	−0.46	−0.41	−0.14	−0.18	−0.14	−0.22	−0.20	−0.34	−0.078	−0.17

TABLE 1. Values of K_i and J_i, $i = 1, 2, \ldots, 8$

3.2. *Spheroidal cells*

Since $\alpha_0 \neq 0$ in this case, we must calculate the contributions to $f^{(1)}(\theta, \phi)$ from all the terms involving the rate-of-strain tensor on the right-hand side of (3.1), as specified in (3.2) and (3.3). For each term in each of those equations, the procedure is identical to that adopted in §3.1. Some details are given in Appendix B, and the corresponding contibutions to $\langle \boldsymbol{p} \rangle, \boldsymbol{D}$, etc., are listed below. The contribution to $\langle \boldsymbol{p} \rangle^{(1)}$ is

$$-2\alpha_0(e_{13}J_4, e_{23}J_4, \tfrac{3}{2}e_{33}K_4), \tag{3.14}$$

where J_4, K_4 are defined in (B 10), (B 11). The contribution to $\boldsymbol{D}^{(1)}/V_s^2\tau$ is obtained from (1.15) using (B 12) and (3.14), and is

$$-2\alpha_0\begin{pmatrix} -\tfrac{3}{4}e_{33}K_5+\tfrac{1}{4}(e_{11}-e_{22})J_6 & \tfrac{1}{2}e_{12}J_6 & e_{13}(J_5-K_1J_4) \\ \tfrac{1}{2}e_{12}J_6 & -\tfrac{3}{4}e_{33}K_5-\tfrac{1}{4}(e_{11}-e_{22})J_6 & e_{23}(J_5-K_1J_4) \\ e_{13}(J_5-K_1J_4) & e_{23}(J_5-K_1J_4) & \tfrac{3}{2}e_{33}(K_5-2K_1K_4) \end{pmatrix}, \tag{3.15}$$

where K_5, J_5, J_6 are defined in (B 13).

The contributions to the bulk stress tensor of the terms in $f^{(1)}$ involving the strain rate are again straightforward. There is a symmetric contribution to $\Sigma^{(\mathrm{sd})}$ equal to nS' times the tensor given in (B 12). The part of $\Sigma^{(\mathrm{p})}$ involving $\boldsymbol{L}$ (equation (1.7)) still has an antisymmetric and a symmetric component; the former is equal to

$$-npvhg\alpha_0 J_4\begin{pmatrix} 0 & 0 & e_{13} \\ 0 & 0 & e_{23} \\ -e_{13} & -e_{23} & 0 \end{pmatrix}, \tag{3.16a}$$

while the latter is $-\tfrac{1}{2}npvhg\alpha_0^2$ multiplied by

$$\begin{pmatrix} -\tfrac{3}{4}e_{33}(K_6-2K_4)+\tfrac{1}{4}(e_{11}-e_{22})J_8 & \tfrac{1}{2}e_{12}J_8 & e_{13}(J_7-J_4) \\ \tfrac{1}{2}e_{12}J_8 & -\tfrac{3}{4}e_{33}(K_6-2K_4)-\tfrac{1}{4}(e_{11}-e_{22})J_8 & e_{23}(J_7-J_4) \\ e_{13}(J_7-J_4) & e_{23}(J_7-J_4) & \tfrac{3}{2}e_{33}(K_6-2K_4) \end{pmatrix}, \tag{3.16b}$$

where K_6, J_7, J_8 are given in (B 15). The first-order continuum model is now complete.

4. Stability of a uniform suspension

We now use the new continuum model to examine the stability of a uniform basic state in which there is no bulk motion and the cell concentration is n_0; this is the same problem that was solved by PHK with the old continuum model. The first point of interest is that the deviatoric stress tensor is non-zero in the basic state, although it is of course divergence-free. There are three contributions to this stress, arising from the intrinsic stresslets of the swimming motion ($\boldsymbol{\Sigma}^{(\mathrm{s})(0)}$), from the diffusive stress ($\boldsymbol{\Sigma}^{(\mathrm{d})(0)}$), and from the external couples ($\boldsymbol{\Sigma}^{(L)(0)}$). We write the combination as $\rho V_{\mathrm{s}}^2 \boldsymbol{\Sigma}^{(0)}$, where the dimensionless $\boldsymbol{\Sigma}^{(0)}$ is given by

$$\boldsymbol{\Sigma}^{(0)} = \tfrac{1}{3}\chi_1 K_3\left(1-\frac{3\alpha_0}{2\lambda}\chi_2\right)\begin{pmatrix} -1 & 0 & 0 \\ 0 & -1 & 0 \\ 0 & 0 & 2 \end{pmatrix}, \tag{4.1}$$

where

$$\chi_1 = n_0 S'/\rho V_{\mathrm{s}}^2, \quad \chi_2 = \rho v h g/S', \tag{4.2}$$

from (2.14*a*) and (2.15). Note that S' is given by (2.13), (1.12*a*) and (1.12*c*); if we use parameter values for *C. nivalis*, as given in PHK, plus $\lambda = 2.2$, and estimate the distance $l\cos\gamma$ (figure 3) to be b, we find that the ratio $3\alpha_0\chi_2/2\lambda$ is approximately 3.2×10^{-3}, so the factor in (4.1) is positive. It also turns out that the diffusive contribution to S' (equation (2.13)) is only about 1 % of S and is therefore negligible.

For the stability analysis, the variables are non-dimensionalized using timescale B, velocity scale V_{s}, lengthscale BV_{s}, pressure/stress scale ρV_{s}^2 and concentration scale n_0. We then write

$$n = 1+\epsilon n', \quad \boldsymbol{u} = \epsilon \boldsymbol{u}', \quad p_{\mathrm{e}} = p_{\mathrm{e}0}+\epsilon p_{\mathrm{e}}', \quad \boldsymbol{\Sigma} = \boldsymbol{\Sigma}^{(0)}+\epsilon\boldsymbol{\Sigma}',$$

where ϵ is a small parameter. As a consequence of the non-dimensionalization, the scale for leading-order vorticity and strain rate is ϵ/B, so this ϵ is the same as that defined in (2.2); thus $\langle\boldsymbol{p}\rangle = \langle\boldsymbol{p}\rangle^{(0)}+\epsilon\langle\boldsymbol{p}\rangle^{(1)}$, etc. The linearized governing equations (1.1)–(1.3) are now

$$\nabla\cdot\boldsymbol{u}' = 0, \tag{4.3}$$

$$\frac{\partial \boldsymbol{u}'}{\partial t} = -\nabla p_{\mathrm{e}}' - \beta n'\boldsymbol{k} + \nabla\cdot\boldsymbol{\Sigma}', \tag{4.4}$$

$$\frac{\partial n'}{\partial t} = -\nabla\cdot\langle\boldsymbol{p}\rangle^{(1)} - \langle\boldsymbol{p}\rangle^{(0)}\cdot\nabla n' + \nabla\cdot(\boldsymbol{D}^{(0)}\cdot\nabla n'), \tag{4.5}$$

where

$$\beta = n_0 v B g\Delta\rho/V_{\mathrm{s}}\rho \tag{4.6}$$

and $\boldsymbol{D}^{(0)}$ is the dimensionless version of the zero-order diffusivity tensor defined by (2.11), so it has the multiplier τ/B instead of $V_{\mathrm{s}}^2\tau$. We note that the first-order correction to $\boldsymbol{D}$ does not come into the stability analysis at this order, so the assumption of just two diffusivities, horizontal and vertical, as in the model of Childress *et al.* (1975), is indeed justified. The vectors $\langle\boldsymbol{p}\rangle^{(0)}$ and $\langle\boldsymbol{p}\rangle^{(1)}$ are given by (2.8) and a combination of (3.9*a*) with (3.14). Thus the cell conservation equation (4.5) becomes

$$\frac{\partial n'}{\partial t} + K_1\frac{\partial n'}{\partial z} - \left[D_{\mathrm{H}}\left(\frac{\partial^2 n'}{\partial x^2}+\frac{\partial^2 n'}{\partial y^2}\right)+D_{\mathrm{V}}\frac{\partial^2 n'}{\partial z^2}\right]$$
$$= -J_1\left(\frac{\partial\omega_2}{\partial x}-\frac{\partial\omega_1}{\partial y}\right) + 2\alpha_0 J_4\left(\frac{\partial e_{13}}{\partial x}+\frac{\partial e_{23}}{\partial y}\right) + 3\alpha_0 K_4\frac{\partial e_{33}}{\partial z}, \tag{4.7}$$

where $D_{\mathrm{H}} = (\tau/B)K_1/\lambda$, $D_{\mathrm{V}} = (\tau/B)K_2$.

It remains now to specify Σ', which can be calculated from (1.13), (1.11), (1.12*b*), (1.7), (2.10), (2.16), (3.13) and (3.16). This perturbation stress tensor can be written as the sum of four terms, the original Newtonian term (1.6), a term due to the non-zero stress in the basic state, an antisymmetric term (from the $\boldsymbol{\varepsilon}\cdot\langle \boldsymbol{L}\rangle$ term in (1.7)) and a symmetric term. Thus we have

$$\Sigma' = \frac{2\boldsymbol{e}}{R} + \Sigma^{(0)} n' + \tfrac{1}{2}\chi_1 \chi_2 \Sigma^{a} + \Sigma^{b}, \tag{4.8}$$

where $\Sigma^{(0)}$ is given in (4.1), χ_1, χ_2 are defined in (4.2),

$$R = \rho V_{\mathrm{s}}^2 B/\mu \tag{4.9}$$

is a sort of cell Reynolds number, and Σ^{a}, Σ^{b} are defined below:

$$\Sigma^{a} = \begin{pmatrix} 0 & 0 & J_1\omega_2 - 2\alpha_0 J_4 e_{13} \\ 0 & 0 & -J_1\omega_1 - 2\alpha_0 J_4 e_{23} \\ -J_1\omega_2 + 2\alpha_0 J_4 e_{13} & J_1\omega_1 + 2\alpha_0 J_4 e_{23} & 0 \end{pmatrix} \tag{4.10}$$

and

$$\Sigma^{b} = \begin{pmatrix} Ae_{33} + C(e_{11} - e_{22}) & 2Ce_{12} & -2Ge_{13} + F\omega_2 \\ 2Ce_{12} & Ae_{33} - C(e_{11} - e_{22}) & -2Ge_{23} - F\omega_1 \\ -2Ge_{13} + F\omega_2 & -2Ge_{23} - F\omega_1 & -2Ae_{33} \end{pmatrix}. \tag{4.11}$$

Here the constants A, C, F, G are given in full in Appendix C, together with their estimated values for *C. nivalis*. Each of these constants contains one term proportional to χ_1, representing the intrinsic swimming stresslets (together with the small contribution from rotary diffusion), a term proportional to $\chi_1\chi_2$, representing the external couples, and (with the exception of F) a term proportional to nv/R, representing the 'Batchelor stresses' of the first part of (1.7). This last term involves each of the four constants $\alpha_1 - \alpha_4$ (Appendix A), of which only the α_3 term has a simple interpretation: it is equivalent to a small increase in viscosity of the suspension.

Even without evaluating the complicated functions of α_0 and λ that are involved in the coefficients of Σ', we can estimate the values of the dimensionless constants R^{-1}, χ_1, χ_2, $n_0 v$, β, using the dimensional data given in table 1 of PHK, except that we use $V_{\mathrm{s}} = 63\ \mu\mathrm{m\ s^{-1}}$, as derived above, instead of $100\ \mu\mathrm{m\ s^{-1}}$ as used there. They are

$$R^{-1} \approx 73, \quad \chi_1 \approx 8.1, \quad \chi_2 \approx 1.5 \times 10^{-2}, \quad n_0 v \approx 5 \times 10^{-4}, \quad \beta \approx 13.$$

The other remaining dimensionless constant is τ/B, which comes into the diffusivity (B/τ is a Péclet number); with $\tau = 1.3$ s (Häder & Hill 1990) and $B = 3.4$ s (PHK), $\tau/B \approx 0.38$. The above numbers indicate that the leading contributions to the symmetric stress Σ^{b} are the $O(R^{-1})$ Newtonian term and the $O(\chi_1)$ intrinsic stresslet term; the $O(n_0 v/R)$ Batchelor stress, in particular, is negligible. The numerical values of the constants (e.g. Appendix C) do not alter these conclusions. Of the other terms in (4.8), the $\Sigma^{(0)}n'$ term ($\propto \chi_1$) is not small, but the antisymmetric term is small; we retain it, however, in case it introduces any qualitatively new effects into the stability analysis.

As in PHK, the governing equations are linear differential equations with constant coefficients, so we can examine stability in terms of individual Fourier modes. We therefore rewrite all perturbation quantities in the form (for example)

$$n'(x, y, z, t) = N \exp\left[\sigma t + \mathrm{i}(kx + ly + mz)\right],$$

substitute in the equations and eliminate the amplitudes (N, etc.) to leave a dispersion relation for the growth rate σ in terms of the (dimensionless) wavenumbers k, l, m. The dispersion relation derived in PHK, in the present notation, was the quadratic equation

$$[\sigma + \mathrm{i}m + D_*(k^2+m^2)]\left[\sigma + \frac{k^2+m^2}{R}\right] = \beta\frac{k^2}{k^2+m^2}[(1-\alpha_0)k^2 + (1+\alpha_0)m^2], \tag{4.12}$$

where without loss of generality we have taken $l = 0$ and D_* is the dimensionless isotropic diffusivity.

Each new aspect of the present model affects a different term in (4.12). The first bracket on the left-hand side comes from the left-hand side of (4.7), and therefore becomes

$$\sigma + \mathrm{i}K_1 m + D_{\mathrm{H}}k^2 + D_{\mathrm{V}}m^2; \tag{4.13}$$

the right-hand side of (4.7) leads to the square bracket on the right-hand side of (4.12) becoming

$$(J_1 + \alpha_0 J_4)k^2 + (J_1 - \alpha_0 J_4 + 3\alpha_0 K_4)m^2. \tag{4.14}$$

Remaining changes all come from the $\boldsymbol{\nabla}\cdot\boldsymbol{\Sigma}'$ term in (4.4). The non-zero basic-state stress causes β to be replaced by

$$\beta - \mathrm{i}m\chi_1 K_3\left(1 - \frac{3\alpha_0}{2\lambda}\chi_2\right), \tag{4.15}$$

while the factor $\sigma + (k^2+m^2)/R$ is affected by both $\boldsymbol{\Sigma}^a$ and $\boldsymbol{\Sigma}^b$ and becomes

$$\sigma + \frac{k^2+m^2}{R} + (G+F)k^2 + (G-F)m^2 + \frac{m^2k^2}{k^2+m^2}(3A - 4G - C - 2F)$$
$$-\tfrac{1}{2}\chi_1\chi_2[(J_1+\alpha_0 J_4)k^2 + (J_1 - \alpha_0 J_4)m^2]. \tag{4.16}$$

Thus the dispersion relation is still a quadratic equation for σ; the introduction of new effects has not caused any mode-splitting, merely quantitative changes in the values of σ and of the critical and most unstable wavenumbers. Details can either be computed directly for particular parameter values, or discussed in particular limits, as was done by PHK. Having retained the antisymmetric stress term to see if it had any qualitative effect (such as mode-splitting), we can now see that it does not, and contributes only the small $\chi_1\chi_2$ term in (4.16). We therefore neglect it from now on.

(i) *No vertical variation*: $m = 0$. In this case the roots of the quadratic equation are

$$\sigma = \tfrac{1}{2}k^2\left[-\left(D_{\mathrm{H}} + \frac{1}{R} + G + F\right) \pm \left\{\left(D_{\mathrm{H}} + \frac{1}{R} + G + F\right)^2 + \frac{4\beta(J_1+\alpha_0 J_4)}{k^2}\right.\right.$$
$$\left.\left. - 4D_{\mathrm{H}}\left(\frac{1}{R} + G + F\right)\right\}^{\frac{1}{2}}\right], \tag{4.17}$$

where the largest term in the constant $G+F$ is

$$G + F \approx \chi_1(J_2 + \alpha_0 J_5)$$

from Appendix C. Thus one root is positive, indicating instability, if and only if k is less than the critical value k_{c}, given by

$$k_{\mathrm{c}}^2 = \frac{\beta(J_1 + \alpha_0 J_4)}{D_{\mathrm{H}}\left[\dfrac{1}{R} + \chi_1(J_2 + \alpha_0 J_5)\right]}. \tag{4.18a}$$

Moreover, the positive root is greatest, giving the most unstable disturbance, when $k = k_{\mathrm{m}}$ where

$$\left(\frac{k_{\mathrm{m}}}{k_{\mathrm{c}}}\right)^2 = \frac{D_{\mathrm{H}}^{\frac{1}{2}}\left[\frac{1}{R}+\chi_1(J_2+\alpha_0 J_5)\right]^{\frac{1}{2}}}{\left\{D_{\mathrm{H}}^{\frac{1}{2}}+\left[\frac{1}{R}+\chi_1(J_2+\alpha_0 J_5)\right]^{\frac{1}{2}}\right\}^2}. \qquad (4.18b)$$

The dimensionless growth rate of the most unstable disturbance is

$$\sigma_{\mathrm{m}} = \beta(J_1+\alpha_0 J_4)\left\{D_{\mathrm{H}}^{\frac{1}{2}}+\left[\frac{1}{R}+\chi_1(J_2+\alpha_0 J_5)\right]^{\frac{1}{2}}\right\}^{-2}. \qquad (4.18c)$$

The corresponding results from (4.12), as derived by PHK, are

$$k_{\mathrm{c}}^2 = \frac{\beta(1-\alpha_0)}{D_*/R}, \quad \left(\frac{k_{\mathrm{m}}}{k_{\mathrm{c}}}\right)^2 = \frac{(D_*/R)^{\frac{1}{2}}}{(D_*^{\frac{1}{2}}+R^{-\frac{1}{2}})^2}, \quad \sigma_{\mathrm{m}} = \frac{\beta(1-\alpha_0)}{(D_*^{\frac{1}{2}}+R^{-\frac{1}{2}})^2}. \qquad (4.19)$$

Differences between the present and former results stem from (*a*) the value of D_{H} relative to D_* (β and R being unchanged), as well as (*b*) the values of the constants $J_1+\alpha_0 J_4$ and $J_2+\alpha_0 J_5$. (*a*) D_* is the diffusivity used by PHK (10^{-4} cm^2 s^{-1}) made dimensionless by $V_{\mathrm{s}}^2 B$, so $D_* \approx 0.74$, while $D_{\mathrm{H}} = (\tau/B)(K_1/\lambda) \approx 0.10$. (*b*) We see from table 1 that, for the values of λ quoted, J_1 and J_2 are positive, while J_4 and J_5 are negative. However, the magnitude of J_4 is less than that of J_1, and α_0 lies between 0 and 1, so k_{c}^2 is certainly positive; on the other hand, the magnitude of J_5 can exceed that of J_2, so $J_2+\alpha_0 J_5$ would be negative if α_0 were large enough and λ small enough. Using our best estimates for *C. nivalis* ($\lambda = 2.2$, $\alpha_0 = 0.31$), we obtain $J_2+\alpha_0 J_5 \approx 0.12$; coupled with the fact that $\chi_1 R \approx 0.11$, this is equivalent to a small decrease in Reynolds number, with an insignificant effect on the quantitative results. On the other hand, $J_1+\alpha_0 J_4 \approx 0.37$, which is significantly less than $1-\alpha_0 \approx 0.69$. The net effect on the estimate for k_{c}^2, however, is dominated by the fact that the measured diffusivity is much less than that assumed by PHK ($D_{\mathrm{H}} < D_*$): (4.18*a*) gives $k_{\mathrm{c}}^2 \approx 0.65$, while (4.19*a*) gives $k_{\mathrm{c}}^2 = 0.17$. The estimate for $(k_{\mathrm{m}}/k_{\mathrm{c}})^2$ is reduced from 0.083 (PHK) to 0.034, and the predicted dimensionless maximum growth rate σ_{m} is also reduced, from 0.10 (PHK) to 0.057.

These dimensionless results translate into predictions of dimensional wavelength λ_{m}^* and growth rate σ_{m}^* of the most unstable disturbance as follows:

$$\lambda_{\mathrm{m}}^* = 2\pi B V_{\mathrm{s}}/k_{\mathrm{m}} \approx 9.0 \text{ mm}, \quad \sigma_{\mathrm{m}}^* = \sigma_{\mathrm{m}}/B \approx 0.017 \text{ s}^{-1},$$

compared with 11 mm and 0.029 s^{-1} from the PHK values. In fact, this estimate of most unstable wavelength is exactly the same as that quoted by PHK, as a result of the fact that the estimate of V_{s} used there (100 μm s^{-1}) is greater than the measured value (63 μm s^{-1}) used in the scalings here. The conclusion must therefore be the same as that deduced in the earlier paper: the fact that observed bioconvection patterns have a smaller wavelength (1–3 mm; Kessler 1986*a*) than predicted is most likely to be a consequence of nonlinear factors that do not arise in the linear stability theory.

We may note here that the predicted growth rate σ_{m}^* is substantially smaller than the estimate of D_{r} (0.13 s^{-1}) made in §2. Thus the assumption that it is sufficient to find quasi-steady solutions of the Fokker–Planck equation (1.16) is justified, for estimating not only the critical wavenumber k_{c}, but also the details of the most unstable disturbance.

(ii) *Non-zero vertical wavenumber*. The first point to make is that, when $m \neq 0$, the roots of the quadratic equation are inevitably complex on account of the imaginary terms in (4.13) and (4.15). This means that single modes with non-zero m propagate as growing (or decaying) waves in the positive or negative z-direction. This point was missed by PHK, although there is an im term in (4.12); this term, like the corresponding i$K_1 m$ in (4.13), arises from the fact that the micro-organisms swim upwards, on average. The imaginary term in (4.15) arises from the non-zero basic state stress.

We can deduce both the direction of propagation of three-dimensional disturbances, and whether they are more unstable than those with $m = 0$, by making use of the large magnitude of R^{-1} compared with χ_1, D_{H} and other $O(1)$ quantities in the quadratic equation ($R^{-1} \gg \chi_1$ essentially because the suspension is dilute, and $R^{-1} \gg D_{\mathrm{H}}$ because the kinematic viscosity greatly exceeds the cell diffusivity). Scalings for k and σ are suggested by the above results with $m = 0$. Thus, we take $R \ll 1$ with

$$k^2 = R\kappa^2, \quad m = R\bar{m}, \quad \sigma = R\sigma_1 + R^2\sigma_2 + \dots .$$

Substitution into the quadratic equation gives

$$\sigma_1 = \beta(J_1 + \alpha_0 J_4) - D_{\mathrm{H}}\kappa^2 - \mathrm{i}\bar{m}K_1, \tag{4.20}$$

which is the same result as (4.17), suitably scaled and with $m \neq 0$. The sign of the imaginary term shows immediately that disturbances with $m \neq 0$ propagate upwards, in the positive z-direction, and this leading imaginary term comes from upswimming alone.

At the next order in R we obtain

$$\sigma_2 = -D_{\mathrm{V}}\bar{m}^2 - \left[\beta(J_1 + \alpha_0 J_4)\left\{\frac{\sigma_1}{\kappa^2} + \chi_1(J_2 + \alpha_0 J_5)\right\}\right. \\ \left. + \beta\frac{\bar{m}^2}{\kappa^2}(J_1 + 3\alpha_0 J_4 - 3\alpha_0 K_4) + \mathrm{i}\bar{m}\chi_1 K_3(J_1 + \alpha_0 J_4)\right]. \tag{4.21}$$

We note first that the imaginary term in (4.21), arising from the non-zero basic-state stress, has the same sign as that in (4.20) and is therefore also associated with upwards-propagating disturbances. Next, if all the bracketed coefficients are positive, the real part of σ_2 is negative and the leading effect of non-zero $\bar{m}$ on the growth rate is to reduce it: three-dimensional disturbances are stabilizing. The only way the introduction of non-zero $\bar{m}$ could be destabilizing would be if the coefficient $J_1 + 3\alpha_0(J_4 - K_4)$ were negative, but the results in table 1 indicate that both J_1 and $J_4 - K_4$ are positive, at least for the range of λ values used here. We therefore conclude that, in practice, the most unstable disturbances have zero vertical wavenumber. This conclusion is different from that obtained in PHK because in the old model $J_1 + 3\alpha_0(J_4 - K_4)$ was replaced by $1 - 3\alpha_0$, which could be negative if $\alpha_0 > \frac{1}{3}$. It may be, of course, that this coefficient could change sign for large λ, but the J_i have not been computed for $\lambda \gtrsim \sqrt{10}$.

5. Discussion

It is worth summarizing the major differences between the equations of the new continuum model for suspensions of swimming cells and those of the old one from PHK. There are two differences in the cell conservation equation (1.3): first, the cell-swimming contribution to cell flux, nV_{c}, is not equal to the deterministic value $nV_{\mathrm{s}}\boldsymbol{P}$, but to $nV_{\mathrm{s}}\langle\boldsymbol{p}\rangle$, and secondly, cell diffusion is represented by the tensor $\boldsymbol{D}$, given by (1.15), which is not isotropic. In the limit of zero ambient flow, V_{c} is of course directed vertically upwards, but has a magnitude, $K_1 V_s$, which depends on the value of λ, but is significantly less than V_s; when there is weak ambient flow V_c is not vertical, representing gyrotaxis, but is closer to the vertical than $\boldsymbol{P}$ is. Similarly, for zero ambient flow $\boldsymbol{D}$ is orthotropic, with horizontal diffusivity exceeding the vertical (equation (2.12)). Even for a weak ambient flow, however, none of the vectors $\boldsymbol{k}$, $\langle \boldsymbol{p} \rangle$ or $\boldsymbol{P}$ is an eigenvector of $\boldsymbol{D}$.

All differences in the momentum equation arise from modifications to the stress tensor. For dilute suspensions, both the symmetric and antisymmetric Batchelor stresses (1.7) are negligible compared with the distribution of stresslets associated with the cell's intrinsic swimming motions, $\Sigma^{(s)}$, in equation (1.12*b*). This consists of a non-zero basic-state stress even in a uniform suspension, plus a perturbation that is linear in the local vorticity and strain rate (when these are small). This perturbation is smaller than the basic Newtonian stress, but not negligibly so for the cells of major interest here.

It should be emphasized that the rotational diffusivity, D_r, which arises in the Fokker–Planck equation (1.6), is not tied in a direct mechanical manner to temperature like that arising from Brownian motion (as expressed by the Einstein relation (1.19)). Instead, it is related to the operation of the algal cell. One may think of such a cell as an automaton (in that it can go on swimming for long periods, drawing upon its stored energy) whose mean direction of locomotion is guided by environmentally supplied forces and torques, and where the variance around the mean is due to internally generated stochastic impulses which affect the cells' propulsion apparatus. It may indeed turn out, when the cells have been studied more intensively, that the diffusion constant in the Fokker–Planck equation is not a scalar quantity but it too, like $\boldsymbol{D}$, may be a tensor.

It will be desirable to apply the present model to the other stability problem that has been formulated in the context of bioconvection, that of a layer of finite depth in which the upswimming of cells is coupled with cell diffusion to generate a density stratification that is unstable if the Rayleigh number is large enough, even without the further destabilizing effect of gyrotaxis. This was the problem studied by Childress *et al.* (1975) and by Hill, Pedley & Kessler (1989). The latter paper, in particular, reveals that different modes can be (*a*) critical and (*b*) most unstable at different parameter values, suggesting that a weakly nonlinear theory would be of considerable interest. Thus, not only should we repeat that linear theory with the present model, but we should also extend the model to second or third order in ϵ. That will be feasible only if we eliminate some of the more complex terms in advance, by neglecting small terms and possibly restricting attention to spherical cells ($\alpha_0 = 0$) from the start.

To analyse either the fully nonlinear bioconvention patterns that are observed, or the collective motions that arise in other experiments (e.g. the focused beam of cells on the axis of downwardly directed Poiseuille flow (Kessler 1985*a*), it will be necessary to consider values of ϵ that are not small at all. The only limit that offers hope of analytical progress is that in which either λ or ϵ (or both) is taken to be large, with the other at least $O(1)$. This is a singular limit, corresponding to the case of weak Brownian motion, which formed the subject of several papers by Hinch and Leal (e.g. 1972*a*, *b*; Leal & Hinch 1971). Otherwise, the Fokker–Planck equation (2.1) will require solution in the form of a doubly infinite series of spherical harmonics.

The large-ϵ limit corresponds to a case in which the randomness in cell orientation is weak, and it might be supposed that the resulting continuum model would resemble the earlier one of deterministic gyrotaxis (PHK). However, there was one weakness in that model, which would now disappear; that was the restriction to flows in which the viscous torque on a cell did not so far exceed the gravitational torque as to cause the cells constantly to tumble and to have a stable, quasi-steady orientation. In other words, that model required $\epsilon \lesssim 1$; in following Hinch & Leal (1972*b*) we shall recognize that the cell orientation vector can follow an almost closed orbit in $\boldsymbol{p}$-space (corresponding to cycloidal orbits of the cell centre (Kessler 1985*b*)), and this can be analysed. Thus, despite the tumbling, there will be a specific, steady $\langle \boldsymbol{p} \rangle$, for example.

Other aspects of the cell suspension that require further study include the following:

(i) *Time-dependence* The analysis of time-dependent flows whose timescale is not much greater than D_r^{-1}, so that the $\partial f/\partial t$ term should not be neglected in (1.16).

(ii) *Cell–cell interactions* As the cell concentration increases, the frequency of cell–cell interactions (or 'collisions') will also increase, and the 'mean-free path', i.e. the length of a cell's trajectory between collisions, will decrease. This will lead to a reduction in the magnitude of cell diffusivities, as pointed out by Kessler (1986*a*). Indeed, the data of Häder & Hill (1990) seem to show such a trend, albeit over a small range of concentrations (5×10^5–2×10^6 cells cm^{-3}). More frequent changes of direction can presumably be modelled by an increase in the effective rotational diffusivity, D_r, and hence by a decrease in λ and a consequent reduction in the mean vertical velocity V_c. These are all effects on the cell conservation equation. The momentum equation will be influenced directly by the increase in concentration through the negative buoyancy term (β, equation (4.6)) and through the increased relative importance of the intrinsic stresslet term (χ_1, equation (4.2)). It will also be influenced indirectly by changes to the Batchelor stresses (1.7), but since these are so small compared to the intrinsic stresses, it will not be a high priority to compute them (the complexity of the problem can be seen from, for example, Batchelor & Green (1972) and Batchelor (1977) for not-quite-dilute suspensions of inert spheres).

(iii) *Effects of flagella* Probably much more important is the fact that the swimming cells are not pure spheroids, because of the flagella that propel them. The presence of the flagella will influence both the magnitude of the viscous torque exerted on the cell by the ambient vorticity and strain rate and the rate at which the cell axis tends to reorient itself when it is perturbed from its equilibrium direction $\boldsymbol{P}$. Both these effects will involve a change in equation (1.17), and their quantitative evaluation will require a detailed analysis of the low-Reynolds-number hydrodynamics of the locomotion of the cells in question. Such an analysis will also be necessary in order to provide a more careful evaluation of the intrinsic stresslet contribution to the stress tensor (equation (1.12)).

(iv) *Microgravity* A good test and application of the present model would be to investigate the same species (*C. nivalis*) with different values of λ. This can be achieved by conducting experiments in different gravitational fields, so g and hence β are modified. A microgravity environment would be required to investigate a case with small λ, dominated by randomness in the cell swimming. Note that it is straightforward to adapt the theory for $\epsilon = O(1)$ when $\lambda \ll 1$, corresponding to the case of strong Brownian motion from Brenner & Weissman (1972) for example. A centrifuge could be used to increase λ, although one would have to remember that if g were increased too far, the neglected sedimentation velocity would become comparable with the cell swimming speed.

In this paper, we have developed and applied the new continuum model with bottom-heavy biflagellate algae in mind. However, there is no reason to limit the application either to such organisms or to the single reorienting couple of gravity. Many species of micro-organism, including many bacteria, are *chemotactic*, in that they tend to swim up (or down) concentration gradients of (say) oxygen, nutrients or metabolites. Thus one can replace gravity in the theory by the concentration gradient (Kessler 1989), though we have no *a priori* way of estimating the magnitude of the restoring couple, and hence the effective value of B. However, measurements such as those of Häder & Hill (1990) or Berg & Brown (1972) could be used, together with the results of our theory, to determine it. (See also Keller & Segel 1971 for a similar approach to chemotaxis.)

A more complicated problem is that of modelling *phototactic* micro-organisms, that is cells (such as many algae) that tend to swim towards (or away from) the light. In this case, quite apart from not knowing B, it is not easy to give a quantitative specification of the light to which the cells respond, since there may be different direct and diffuse components, depending, for example, on the weather and the turbidity of the water in which the cells live. In particular, the intensity of light at a point may depend on the concentration of the cells themselves, not just locally but over a considerable region.

A further interesting development would be to apply the model to species in addition to *Chlamydomonas* (e.g. *Dunaliella* or *Volvox*), which respond to two different orienting torques, say both gravity and light. Different relative orientations of the two external fields would lead to a different behaviour, the experimental study of which in a variety of species would be very revealing.

We are particularly grateful to N. A. Hill for many helpful comments and for providing the preliminary data from Häder & Hill (1990), to O. E. Jensen for plotting figure 4, to J. F. Brady, H. Brenner and L. G. Leal for useful discussions, and to G. K. Batchelor, who made a comment that initially put us on the right track with this theory. The work was done while T.J.P. was on sabbatical leave in the Physics Department at the University of Arizona, and he is extremely grateful to that Department and to the Center for the Study of Complex Systems for facilities and for financial support.

Appendix A

Letting $r = a/b$, so that $\alpha_0 = (r^2-1)/(r^2+1)$, the constants $\alpha_{1,2,3,4}$ in (1.7), α_5 in (1.11), α_F in (1.12*a*) and $\alpha_\perp$ in (1.18) are defined as follows (from Jeffery 1922 via Batchelor 1970 and Leal & Hinch 1971; see also Brenner 1974); the values quoted are for $r = 1.38$ ($\alpha_0 = 0.31$):

$$\alpha_1 = \frac{1}{I_1}\left(1+\frac{L_1}{L_2}-\frac{2I_1}{I_2}\right) = 0.135, \quad \alpha_2 = -\frac{1}{I_1}\left(1-\frac{I_1}{I_2}\right) = 0.122,$$

$$\alpha_3 = \frac{1}{I_1} = 1.15, \qquad \alpha_4 = \frac{1}{3I_1}\left(1-\frac{L_1}{L_2}\right) = -0.127,$$

$$\alpha_5 = \frac{6(r^4-1)}{2r^2I_2+(r^2+1)^2L_2} = 3.16, \quad \alpha_\perp = \frac{2(r^2+1)}{3(r^2-1)}\alpha_5 = 6.80,$$

where

$$I_1 = \int_0^\infty \frac{2r\,\mathrm{d}\lambda}{(r^2+\lambda)^{\frac{1}{2}}(1+\lambda)^3} = \frac{r^2(2r^2-5+3\gamma)}{2(r^2-1)^2} = 0.866,$$

$$I_2 = \int_0^\infty \frac{r(r^2+1)\,\mathrm{d}\lambda}{(r^2+\lambda)^{\frac{3}{2}}(1+\lambda)^2} = \frac{(r^2+1)\,(r^2+2-3r^2\gamma)}{(r^2-1)^2} = 0.783,$$

$$L_1 = \int_0^\infty \frac{r\lambda\,\mathrm{d}\lambda}{(r^2+\lambda)^{\frac{1}{2}}(1+\lambda)^3} = \frac{r^2[2r^2+1-\gamma(4r^2-1)]}{4(r^2-1)^2} = 0.315,$$

$$L_2 = \int_0^\infty \frac{r\lambda\,\mathrm{d}\lambda}{(r^2+\lambda)^{\frac{3}{2}}(1+\lambda)^2} = I_1-2L_1 = 0.237,$$

and

$$\gamma = \frac{\cosh^{-1} r}{r(r^2-1)^{\frac{1}{2}}}.$$

Also $\alpha_{\mathrm{F}} \approx 1.08$ (Happel & Brenner 1965).

Appendix B. Contribution to the first-order averages involving *e*

In view of (3.1) and (3.2), we write this contribution as

$$f^{(1)} = -2\alpha_0\lambda\mu\{\tfrac{3}{4}e_{33}\,g_2(x)+e_{13}\,g_3(x)\cos\phi+e_{23}\,g_3(x)\sin\phi \\ +\tfrac{1}{2}(e_{11}-e_{22})\,g_4(x)\cos 2\phi+e_{12}\,g_4(x)\sin 2\phi\}, \quad \text{(B 1)}$$

and the functions g_2, g_3, g_4 satisfy the equations

$$\mathscr{L}g_2 = 2\,\mathrm{e}^{\lambda x}[-\lambda x(1-x^2)+3x^2-1], \quad \text{(B 2)}$$

$$\mathscr{L}g_3-\frac{g_3}{1-x^2} = \mathrm{e}^{\lambda x}(1-x^2)^{\frac{1}{2}}[\lambda(2x^2-1)+6x], \quad \text{(B 3)}$$

$$\mathscr{L}g_4-\frac{4g_4}{1-x^2} = \mathrm{e}^{\lambda x}(1-x^2)\,(\lambda x+3), \quad \text{(B 4)}$$

where

$$\mathscr{L}g = \frac{\mathrm{d}}{\mathrm{d}x}[(1-x^2)\,g']-\lambda\frac{\mathrm{d}}{\mathrm{d}x}[(1-x^2)\,g].$$

The solution of (B 2) is

$$g_2 = \mathrm{e}^{\lambda x}(1-x^2-2K_1/\lambda), \quad \text{(B 5)}$$

where K_1 is given by (2.9) and the normalization condition $\int_{-1}^{1} g_2\,\mathrm{d}x = 0$ has been used. Equation (B 3) has exactly the same form as (3.4), apart from a different right-hand side. The solution is

$$g_3 = \sum_{n=0}^{\infty} \lambda^n \sum_{r=1}^{n+2} \tilde{a}_{n,r} P_r^1(x), \quad \text{(B 6)}$$

where $\tilde{a}_{n,r} = 0$ if $n+r$ is odd, $\tilde{a}_{0,2} = -\frac{1}{3}$, $\tilde{a}_{1,1} = -\frac{1}{5}$, $\tilde{a}_{1,3} = -\frac{2}{15}$, and the recurrence relation for $\tilde{a}_{n,r}$ is the same as that for $a_{n,r}$ (equation (3.7*a*)), but with $b_{n+1,r}$ replaced by

$$\tilde{b}_{n+1,r} = -\frac{(2r+1)\,\Gamma\left(\dfrac{n+1}{2}\right)\Gamma\left(\dfrac{n+2}{2}\right)(n^2+5n+4+r+r^2)}{16\Gamma(n+1)\,\Gamma\left(\dfrac{n+5-r}{2}\right)\Gamma\left(\dfrac{n+6+r}{2}\right)}. \quad \text{(B 7)}$$

It should be noted that the limits of the sums in (B 6) are different from those in (3.6).

Finally, the solution of (B 4) involves associated Legendre functions $P_r^2(x)$, and it can be written

$$g_4 = \sum_{n=0}^{\infty} \lambda^n \sum_{r=2}^{n+2} \bar{a}_{n,r} P_r^2(x), \tag{B 8}$$

where $\bar{a}_{n,r} = 0$ if $n+r$ is odd, $\bar{a}_{0,2} = -\frac{1}{6}$, $\bar{a}_{1,3} = -\frac{1}{30}$ and

$$\bar{a}_{n+1,r} = \bar{a}_{n,r-1}\frac{(r-2)}{r(2r-1)} - \bar{a}_{n,r+1}\frac{(r+3)}{(r+1)(2r+3)} + \frac{\bar{b}_{n+1,r}}{r(r+1)} \tag{B 9a}$$

with

$$\bar{b}_{n+1,r} = -\frac{(n+4)(2r+1)\,\Gamma\left(\frac{n+2}{2}\right)\Gamma\left(\frac{n+3}{2}\right)}{8\Gamma(n+2)\,\Gamma\left(\frac{n+5-r}{2}\right)\Gamma\left(\frac{n+6+r}{2}\right)}, \tag{B 9b}$$

when $n+r$ is even.

The contribution of these terms to $\langle \boldsymbol{p} \rangle^{(1)}$ is

$$-2\alpha_0(e_{13}J_4, e_{23}J_4, \tfrac{3}{2}e_{33}K_4),$$

where

$$J_4 = \pi\lambda\mu\int_{-1}^{1}(1-x^2)^{\frac{1}{2}}g_3(x)\,\mathrm{d}x = \tfrac{4}{3}\pi\lambda\mu\sum_{l=0}^{\infty}\lambda^{2l+1}\tilde{a}_{2l+1,1}, \tag{B 10}$$

$$K_4 = \pi\lambda\mu\int_{-1}^{1}g_2(x)\,x\,\mathrm{d}x = 1-\coth^2\lambda - 2K_1/\lambda. \tag{B 11}$$

The contribution to $\langle \boldsymbol{pp} \rangle^{(1)}$ is

$$-2\alpha_0\begin{pmatrix} -\frac{3}{4}e_{33}K_5+\frac{1}{4}(e_{11}-e_{22})J_6 & \frac{1}{2}e_{12}J_6 & e_{13}J_5 \\ \frac{1}{2}e_{12}J_6 & -\frac{3}{4}e_{33}K_5-\frac{1}{4}(e_{11}-e_{22})J_6 & e_{23}J_5 \\ e_{13}J_5 & e_{23}J_5 & \frac{3}{2}e_{33}K_5 \end{pmatrix}, \tag{B 12}$$

where

$$K_5 = \pi\lambda\mu\int_{-1}^{1}x^2g_2(x)\,\mathrm{d}x = -\frac{2}{\lambda}\left(2+\frac{5}{\lambda^2}-\frac{4\coth\lambda}{\lambda}-\coth^2\lambda\right), \tag{B 13a}$$

$$J_5 = \pi\lambda\mu\int_{-1}^{1}(1-x^2)^{\frac{1}{2}}xg_3(x)\,\mathrm{d}x = \tfrac{4}{5}\pi\lambda\mu\sum_{l=0}^{\infty}\lambda^{2l}\tilde{a}_{2l,2}, \tag{B 13b}$$

$$J_6 = \pi\lambda\mu\int_{-1}^{1}(1-x^2)\,g_4(x)\,\mathrm{d}x = \tfrac{16}{5}\pi\lambda\mu\sum_{l=0}^{\infty}\lambda^{2l}\tilde{a}_{2l,2}. \tag{B 13c}$$

Finally, the contribution to $\langle 2(\boldsymbol{p}\cdot\boldsymbol{k})\boldsymbol{pp} \rangle^{(1)}$ is

$$-2\alpha_0\begin{pmatrix} -\frac{3}{4}e_{33}(K_6-2K_4)+\frac{1}{4}(e_{11}-e_{22})J_8 & \frac{1}{2}e_{12}J_8 & e_{13}J_7 \\ \frac{1}{2}e_{12}J_8 & -\frac{3}{4}e_{33}(K_6-2K_4)-\frac{1}{4}(e_{11}-e_{22})J_8 & e_{23}J_7 \\ e_{13}J_7 & e_{23}J_7 & \frac{3}{2}e_{33}K_6 \end{pmatrix}, \tag{B 14}$$

where

$$K_6 = 1+\frac{24}{\lambda^2}+\frac{54}{\lambda^4}-\frac{3\coth\lambda}{\lambda}\left(1+\frac{16}{\lambda^2}\right)-\coth^2\lambda\left(1+\frac{6}{\lambda^2}\right) \tag{B 15a}$$

$$J_7 = \tfrac{32}{35}\pi\lambda\mu\sum_{l=0}^{\infty}\lambda^{2l+1}\tilde{a}_{2l+1,3}+\tfrac{2}{5}J_4, \quad J_8 = \tfrac{32}{7}\pi\lambda\mu\sum_{l=0}^{\infty}\lambda^{2l+1}\bar{a}_{2l+1,3}. \tag{B 15b, c}$$

Appendix C. Constants in Σ^b

$$\begin{aligned}
A &= \tfrac{3}{2}\chi_1\alpha_0K_5+\tfrac{3}{8}\chi_1\chi_2\alpha_0^2(K_6-2K_4)+\frac{4n_0v}{R}\left\{\alpha_1K_7+\alpha_4K_3-\alpha_2\frac{K_1}{\lambda}-\frac{\alpha_3}{2}\right\}\\
&= -0.051\chi_1+0.037\chi_1\chi_2-2.38n_0v/R,\\
C &= \chi_1\frac{\alpha_0}{2}J_4-\chi_1\chi_2\frac{\alpha_0^2}{8}J_8+\frac{4n_0v}{R}\left\{\alpha_1\frac{K_3}{\lambda^2}+\alpha_2\frac{K_1}{\lambda}+\frac{\alpha_3}{2}\right\}\\
&= -0.040\chi_1+0.001\chi_1\chi_2+2.32n_0v/R,\\
G &= \chi_1\alpha_0J_5+\chi_1\chi_2\frac{\alpha_0^2}{4}(J_7-J_4)+\frac{4n_0v}{R}\left\{\alpha_1K_8-\frac{\alpha_2}{2}\left(1-\frac{K_1}{\lambda}\right)-\frac{\alpha_3}{2}\right\}\\
&= -0.040\chi_1+0.001\chi_1\chi_2-2.52n_0v/R,\\
F &= \chi_1J_2+\chi_1\chi_2\frac{\alpha_0}{4}(J_3-J_1)=0.16\chi_1-0.026\chi_1\chi_2,
\end{aligned}$$

where $$K_7=\frac{4}{\lambda}\left[\frac{7}{\lambda}+\frac{18}{\lambda^3}-\coth\lambda\left(1+\frac{18}{\lambda^2}\right)\right],\quad K_8=\frac{1}{\lambda}\left[\frac{5}{\lambda}+\frac{12}{\lambda^3}-\coth\lambda\left(1+\frac{12}{\lambda^2}\right)\right].$$

REFERENCES

ARFKEN, G. 1985 *Mathematical Methods for Physicists*, 3rd edn. Academic.

BALOCH, K. M. & VEN, T. G. M. VAN DE 1989 Transient light scattering of suspensions of charged nonspherical particles subjected to an electric field. *J. Colloid Interface Sci.* **129**, 91–104.

BATCHELOR, G. K. 1970 The stress system in a suspension of force-free particles. *J. Fluid Mech.* **41**, 545–570.

BATCHELOR, G. K. 1977 The effect of Brownian motion on the bulk stress in a suspension of spherical particles. *J. Fluid Mech.* **83**, 97–117.

BATCHELOR, G. K. & GREEN, J. T. 1972 The determination of bulk stress in a suspension of spherical particles to $O(c^2)$. *J. Fluid Mech.* **56**, 401–427.

BERG, H. C. & BROWN, D. A. 1972 Chemotaxis in *Escherichia coli* analysed by three-dimensional tracking. *Nature* **239**, 500–504.

BRENNER, H. 1972 Suspension rheology. *Prog. in Heat Mass Transfer* **5**, 89–129.

BRENNER, H. 1974 Rheology of a dilute suspension of axisymmetric Brownian particles. *Intl J. Multiphase Flow* **1**, 195–341.

BRENNER, H. & WEISSMAN, M. H. 1972 Rheology of a dilute suspension of dipolar spherical particles in an external field. II. Effect of rotary Brownian motion. *J. Colloid Interface Sci.* **41**, 499–531.

CHILDRESS, S., LEVANDOWSKY, M. & SPIEGEL, E. A. 1975 Pattern formation in a suspension of swimming micro-organisms. *J. Fluid Mech.* **69**, 591–613.

GRADSHTEYN, I. S. & RYZHIK, I. M. 1980 *Table of Integrals, Series and Products.* (English edn, ed. A. Jeffrey). Academic.

GUELL, D. C., BRENNER, H., FRANKEL, R. B. & HARTMAN, H. 1988 Hydrodynamic forces and band formation in swimming magnetotactic bacteria. *J. Theor. Biol.* **135**, 525–542.

HÄDER, D. & HILL, N. A. 1990 Tracking and averaging the swimming trajectories of *Chlamydomonas nivalis* (in preparation).

HAPPEL, J. & BRENNER, H. 1965 *Low Reynolds Number Hydrodynamics.* Prentice-Hall.

HILL, N. A., PEDLEY, T. J. & KESSLER, J. O. 1989 The growth of bioconvection patterns in a suspension of gyrotactic micro-organisms in a layer of finite depth. *J. Fluid Mech.* **208**, 509–543.

HINCH, E. J. & LEAL, L. G. 1972*a* The effect of Brownian motion on the rheological properties of a suspension of non-spherical particles. *J. Fluid Mech.* **52**, 683–712.

HINCH, E. J. & LEAL, L. G. 1972*b* Note on the rheology of a dilute suspension of dipolar spheres with weak Brownian couples. *J. Fluid Mech.* **56**, 803–813.

JEFFERY, G. B. 1922 The motion of ellipsoidal particles immersed in a viscous fluid. *Proc. R. Soc. Lond.* A **102**, 161–179.

KELLER, E. F. & SEGEL, L. A. 1970 Initiation of slime mold aggregation viewed as an instability. *J. Theor. Biol.* **26**, 399–415.

KELLER, E. F. & SEGEL, L. A. 1971 Model for chemotaxis. *J. Theor. Biol.* **30**, 224–234.

KESSLER, J. O. 1984 Gyrotactic buoyant convection and spontaneous pattern formation in algal cell cultures. In *Nonequilibrium Cooperative Phenomena in Physics and Related Fields* (ed. M. G. Velarde), pp. 241–248. Plenum.

KESSLER, J. O. 1985*a* Hydrodynamic focusing of motile algal cells. *Nature* **313**, 218–220.

KESSLER, J. O. 1985*b* Co-operative and concentrative phenomena of swimming micro-organisms. *Contemp. Phys.* **26**, 147–166.

KESSLER, J. O. 1986*a* The external dynamics of swimming micro-organisms. In *Progress in Phycological Research*, vol. 4 (ed. F. E. Round), pp. 257–307. Bristol Biopress.

KESSLER, J. O. 1986*b* Individual and collective dynamics of swimming cells. *J. Fluid Mech.* **173**, 191–205.

KESSLER, J. O. 1989 Path and pattern – the mutual dynamics of swimming cells and their environment. *Comments Theor. Biol.* **1**, 85–108.

LEAL, L. G. & HINCH, E. J. 1971 The effect of weak Brownian rotations on particles in shear flow. *J. Fluid Mech.* **46**, 685–703.

LEAL, L. G. & HINCH, E. J. 1972 The rheology of a suspension of nearly spherical particles subject to Brownian rotations. *J. Fluid Mech.* **55**, 745–765.

PEDLEY, T. J., HILL, N. A. & KESSLER, J. O. 1988 The growth of bioconvection patterns in a uniform suspension of gyrotactic micro-organisms. *J. Fluid Mech.* **195**, 223–237 (referred to as PHK).

PEDLEY, T. J. & KESSLER, J. O. 1987 The orientation of spheroidal micro-organisms swimming in a flow field. *Proc. R. Soc. Lond.* B **231**, 47–70.

SPORMANN, A. M. 1987 Unusual swimming behaviour of a magnetotactic bacterium. *FEMS Microbiol. Ecol.* **45**, 37–45.